**ORIGINAL PAPER**

# Quantum-mechanical four-body versus semi-classical three-body theories for double charge exchange in collisions of fast alpha particles with helium targets

## Dževad Belkić[1,2]

## Abstract

Within the two-channel distorted wave second-order perturbative theoretical formalism, we study capture of both electrons from helium-like targets by heavy nuclei as projectiles at intermediate and high impact energies. The emphasis is on the four-body single-double scattering (SDS-4B) method and the three-body continuum distorted wave impact parameter method (CDW-3B-IPM). The SDS-4B method deals with the full quantum-mechanical correlative dynamics of all the four interactively participating particles (two electrons, two nuclei). The CDW-3B-IPM is a semi-classical three-body independent particle model (one electron, two nuclei), using a combinatorial calculus to describe double capture by a product of two uncorrelated probabilities, integrated over impact parameters. Both theories share a common feature in having altogether two electronic full Coulomb continuum wave functions. One such function is centered on the projectile nucleus in the entrance channel, whereas the other is centered on the target nucleus in the exit channel. These two methods satisfy the correct initial and final Coulomb boundary conditions in the asymptotic region of scattering, at infinitely large inter-particle separations. Yet, it is presently demonstrated that most of the available experimental data on total cross sections for the double capture from helium by alpha particles distinctly favor the SDS-4B method. This is especially true at intermediate energies. Such energies are critically important in versatile applications under the general umbrella of ion transport in matter, including thermonuclear fusion (plasma physics) and ion therapy (medicine).

**Keywords** Double charge exchange · Correct boundary conditions · Distorted wave methods

---

✉ Dževad Belkić
dzevad.belkic@ki.se

1   Department of Oncology-Pathology, Karolinska Institute, P.O. Box 260, 171 76 Stockholm, Sweden

2   Radiation Physics and Nuclear Medicine, Karolinska University Hospital, P.O. Box 260, 171 76 Stockholm, Sweden

# 1 Introduction

In the present study, we consider second-order two-center perturbative theories for double electron capture by heavy nuclei from helium-like target at intermediate and high impact energies $E$. The use is made of both the correlated and uncorrelated collisional dynamics. The correlated formalism is fully quantum-mechanical with all the four actively participating particles (two electrons, two nuclei). The uncorrelated formalism is a semi-classical independent-particle modeling with three constituents (one electron and two nuclei). This three-body description connects to the actual four-body problem by providing the probability for double capture as the product of two independent single electron probabilities for each impact parameter. Herein, transfer of one electron at a time occurs with no reference whatsoever to what happens to the other electron. In such an independent particle framework, the electronic motion is quantized, while the nuclear motion develops along the classical straight-line impact-parameter dependent trajectories.

These two formalisms satisfy the correct boundary conditions in both the entrance and exit channels of their respective three-body or four-body problems. The theoretical basis of the necessity to take into account the correct boundary conditions for two-electron charge-exchange is well-known [1–8]. Earlier [9–11], the importance of these conditions has conclusively been established for one-electron capture. The reason is in the consistency of the theory for Coulomb collisions involving ions as projectiles and atoms or ions or molecules as targets [7, 8].

For single and double charge exchange, the most frequently utilized perturbative quantum-mechanical theories, in their three-body (3B) and four-body (4B) versions, are the boundary-corrected first Born (CB1), continuum distorted wave (CDW), boundary-corrected continuum intermediate state (BCIS), Born distorted wave (BDW) and continuum-distorted wave—eikonal initial state (CDW-EIS) methods [12–18]. The CB1 method is of the first-order because it describes only one-step single collisions of electrons with nuclei. The CDW, BCIS, BDW and CDW-EIS methods belong to second-order theories on account of including the additional collisions in the intermediate channels, the Thomas-like double-scatterings of the same electron on two nuclei. This two-step mechanism is in both channels (symmetric) of the CDW method, whereas it is in only one channel (asymmetric) of the BCIS, BDW and CDW-EIS methods.

In principle, vastly different choices of distorted waves can be made leading to some symmetric and asymmetric methods. The former methods for double charge exchange use the same type of treatments of motions of both unbound electrons in the field of the projectile and target nuclei in the entrance and exit channels. However, whichever choice is made for distorted waves, they must obey the exact asymptotic behaviors in the scattering region of large inter-particle separations. Moreover, such behaviors ought to be concordant with the short-range perturbation potentials that cause the transitions. Symmetric, two-channel methods can be applied with no need to distinguish between homo-nuclear and hetero-nuclear collisions. On the other hand, when employing asymmetric, one-channel methods, care should be exercised to select the physically appropriate variants (post or prior) depending on the values of the ratio of the projectile and target nuclear charges.

Regarding total cross sections $Q$ for one-electron capture at impact energies $E \geq$ 80 (keV/amu) max$\{\left|\varepsilon_i^T\right|, \left|\varepsilon_f^P\right|\}$, the CB1-3B/4B, CDW-3B/4B, BCIS-3B/4B, BDW-3B/4B and CDW-EIS-3B/4B methods show very good agreement with measurements for multiply charged nuclei impacting on hydrogen-like, helium-like and multi-electron atomic and molecular targets (e.g. H, He, Li, C, N, O, Ne, Ar, Kr, $H_2$, $N_2$, $O_2$, CO, $CO_2$, $CH_4$, $C_2H_4$, $C_2H_6$, $H_2O$, ...) [7, 8]. Here, $\varepsilon_i^T$ and $\varepsilon_f^P$ are the initial and final orbital energies (in atomic units) of an active electron in the Coulomb fields of the nuclear charges of the target (T) and projectile (P), respectively.

Moreover, at the same energies, these methods for single charge exchange are in reasonable mutual agreement for $Q$. Despite being the simplest theory, the CB1-3B/4B method on $Q$ is nevertheless very useful for one-electron transfer since it accurately reproduces the experimental data at intermediate and high $E$. At such energies, the CDW-3B/4B, BCIS-3B/4B, BDW-3B/4B and CDW-EIS-3B/4B methods for one-electron capture are also successful in predicting the reliable values of $Q$.

In contradistinction, for two-electron capture, the CB1-4B, CDW-4B, BCIS-4B, BDW-4B and CDW-EIS-4B methods exhibit uneven performances [3, 19–24]. Thus, for helium targets, the CDW-4B method is successful for impinging protons [19], but not for incident alpha particles [23]. Further, for double capture in the $\alpha-$He collisions, the CB1-4B and CDW-EIS-4B methods fail completely since, at some $E$ within their expected validity domains, they overestimate and underestimate the measured $Q$ by three and four orders of magnitude, respectively [24]. On the other hand, the results for $Q$ from the BCIS-4B and BDW-4B methods [3] lie in a relatively close proximity of the experimental data for two-electron capture by alpha particles from helium targets. It is then clear that two-electron capture processes are markedly sensitive to different choices of distorted waves and distorting potentials.

This runs contrary to a mild sensitivity of single charge exchange to very different selections of distorted waves and distorting potentials. One of the reasons for this occurrence is in the need for a much more pronounced locality condition for two electrons in double than in single electron capture from helium-like targets by nuclei. In double charge exchange at large $E$, the quickly passing projectiles spend very short time near the target and, therefore, two electrons should be in nearly the same place at about the same time to be simultaneously captured. This constraint becomes exacerbated in the methods that employ the identical mechanism for capture of both electrons. As stated, the one-step single collisions of each electron are included in the CB1-4B method when setting up the initial as well as the final total scattering wave functions. Such a constraint makes the CB1-4B method break down at high energies.

By comparison, the BCIS-4B, BDW-4B and CDW-EIS-4B methods for two electron transfer utilize single scatterings in one channel and double scattering in the other channel. In these methods, both electrons undergo the same collisions, either single or double scattering in the entrance or exit channels. In other words, the BCIS-4B, BDW-4B and CDW-EIS-4B methods do not mix single scatterings for one electron with double scatterings for the other electron. However, this type of mixing (or hybridization) of the two mechanisms symmetrically in each channel (entrance, exit) is made in the quantum-mechanical second-order perturbative four-body single-double scattering (SDS-4B) method with the correct initial and final boundary conditions [4, 5]. The

SDS-4B method for the $He^{2+} + He \rightarrow He + He^{2+}$ collisions compares very well with measurements on $Q$, while outperforming the CB1-4B, CDW-4B and CDW-EIS-4B methods. It is also superior to the BCIS-4B and BDW-4B methods below 700 keV for double capture by alpha particles from helium targets.

Specifically, in the SDS-4B method for double charge exchange, each channel contains one electronic full Coulomb wave function for one electron, which undergoes double scatterings on both nuclei (the two-step Thomas mechanism). The other target electron is transferred to the projectile through single scatterings on one nucleus in each channel (the Massey velocity-matching mechanism, i.e the kinematic capture). Thus, in the final state of the system, both electrons become bound to the projectile, albeit by two different pathways (single and double scatterings). As a result, the SDS-4B method takes into account the critically important electron translation factors (ETFs) for two electrons. Furthermore, this method can include the static electron–electron correlations in the initial and/or final bound-state by means of e.g. the configuration-interaction (CI) wave functions.

The semi-classical impact parameter method (IPM) of two electron transfer can be implemented in any theory, including the three-body continuum distorted wave (CDW-3B) method with the ensuing acronym CDW-3B-IPM. Here, the three-body impact parameter dependent transition probabilities are obtained independently for electrons $e_1$ and $e_2$. This means that the probability of capture of e.g. electron $e_1$ in a helium-like target is obtained with no regard to electron $e_2$.

These individual probabilities, being associated with two completely independent uncorrelated events, are multiplied and the ensuing compound probability for capture of both electrons is integrated over all impact parameters to arrive at total cross sections $Q$ [11]. By design, regarding the distortion effects, the CDW-3B-IPM also has two full Coulomb waves, one in each channel centered on different nuclei. Therefore, it is of interest to compare the CDW-3B-IPM and SDS-4B method, as we shall presently do for double charge exchange in the $He^{2+} + He \rightarrow He + He^{2+}$ collisions at intermediate and high energies.

Comparisons for this case as well as for other encounters are necessary in order to establish a practical theory, which could fill in the lacunae in the existing total cross section databases for double charge exchange in ion-atom collisions. Such databases are much in demand as the input quantities to Monte Carlo simulations of energy losses of ions during their passage through matter. These transport phenomena are pivotal, especially to ion plasma in thermonuclear fusion (a powerful new energy source) and to ion therapy (treatment of patients with deep-seated tumors) [7, 8, 25]. For example, reliable total cross sections for double charge exchange in the $He^{2+} - Li$ collisions can provide adequate information about the alpha particle distributions and confinement in hot tokamak plasmas from nuclear fusion reactors [26–29].

Atomic units will be used throughout unless noted otherwise.

## 2 Theory

### 2.1 General link of the undistorted and distorted wave theories

Within the four-body quantum-mechanical spin-independent non-relativistic formalism, double electron capture by a nucleus P from a helium-like target having a nucleus T is schematized via:

$$Z_P + (Z_T; e_1, e_2)_i \longrightarrow (Z_P; e_1, e_2)_f + Z_T. \tag{1}$$
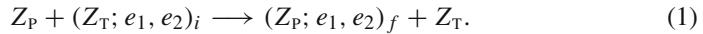
Here, the parentheses symbolize the bound states of electrons $e_1$ and $e_2$, characterized by the standard set $\{i, f\}$ of quantum numbers. The two nuclei in process (1) are heavy and their charges and masses are $Z_{P,T}$ and $M_{P,T} \gg 1$, respectively.

Let the particles $e_1$, $e_2$, P and T be labeled by 1, 2, 3 and 4, respectively. The position vector of the $k$ th particle with respect to the center O of an arbitrary Galilean reference frame XOYZ is denoted by $r_k$ ($k = 1 - 4$). Vectors $x_k$ and $s_k$ are the position vectors of $e_k$ relative to $Z_T$ and $Z_P$, respectively ($k = 1, 2$). Moreover, $R$ is the relative vector of $Z_P$ with respect to $Z_T$. Also, $r_{12}$ is the relative vector of $e_1$ with respect to $e_2$. Further, $r_i$ and $r_f$ are the relative vectors of P and T with respect to the centers-of-masses of the atomic systems $(Z_T; e_1, e_2)_i$ and $(Z_P; e_1, e_2)_f$, respectively. The reduced masses of the entire systems in the entrance and exit channels of process (1) are $\mu_i = M_P(M_T + 2)/M$ and $\mu_f = M_T(M_P + 2)/M$, where $M = M_P + M_T + 2$.

The relationships among these vectors can be written in the following forms:

$$\left. \begin{array}{c} x_1 = r_1 - r_4, \ \ x_2 = r_2 - r_4, \ \ s_1 = r_1 - r_3, \ \ s_2 = r_2 - r_3 \\ R = x_1 - s_1 = x_2 - s_2, \ \ r_{12} = r_1 - r_2, \ \ x_{12} = x_1 - x_2, \ \ s_{12} = s_1 - s_2 \\ r_{12} = x_{12} = s_{12} \end{array} \right\}, \tag{2}$$

$$\left. \begin{array}{c} r_i = r_3 - \dfrac{r_1 + r_2 + M_T r_4}{M_T + 2}, \ \ r_f = r_4 - \dfrac{r_1 + r_2 + M_P r_3}{M_P + 2} \\ r_i = -b' r_f - \dfrac{a'}{\mu_i}(s_1 + s_2), \ \ r_f = -a' r_i - \dfrac{b'}{\mu_f}(x_1 + x_2) \\ a' = \dfrac{M_P}{M_P + 2}, \ \ b' = \dfrac{M_T}{M_T + 2} \end{array} \right\}. \tag{3}$$

Internuclear vector $R$ is resolved into its two components, $R = \rho + v\hat{Z}$. The two-dimensional vector $\rho = (\rho, \phi_\rho)$ is in the scattering (XOY) plane and $\hat{Z}$ is the unit vector of the Z-axis in the XOYZ reference system. Incident vector $v_i \equiv v$ is hereafter set along the Z-axis, implying $\rho \cdot v = 0$. Here, $\rho$ is not an impact parameter vector because, in this Section, only the fully quantum-mechanical theory is used for all the four particles (two electrons and two nuclei).

The initial and final wave vectors $k_{i,f} = \mu_{i,f} v_{i,f}$ are collinear with velocities $v_{i,f}$ of the incident and scattered projectiles, respectively. For heavy nuclei $M_{P,T} \gg 1$, forward scattering prevails so that $v_f \approx v_i \equiv v$. Vector $k_i$ is the momentum vector of P with respect to $(Z_T; e_1, e_2)_i$, whereas $k_f$ is the momentum vector of $(Z_P; e_1, e_2)_f$ relative to T.

The kinetic energy operators $K_i$ and $K_f$ describe the relative motions of the heavy scattering aggregates $Z_P + (Z_T; e_1, e_2)_i$ and $(Z_P; e_1, e_2)_f + Z_T$ in the entrance and exit channels, respectively. The corresponding purely electronic kinetic energy operators are $H_{0T}$ and $H_{0P}$. The total kinetic energy operator $H_0$ for the whole system can be written as the following equivalent expressions in terms of the three sets of the independent variables $\{r_1, r_2, r_3, r_4\}$, $\{x_1, x_2, r_i\}$ or $\{s_1, s_2, r_f\}$:

$$\left.\begin{aligned}
H_0 = K_i + H_{0T}, \ \ K_i = -\frac{1}{2\mu_i}\nabla_{r_i}^2, \ \ H_{0T} = -\frac{1}{2b}\nabla_{x_1}^2 - \frac{1}{2b}\nabla_{x_2}^2 \\
H_0 = K_f + H_{0P}, \ \ K_f = -\frac{1}{2\mu_f}\nabla_{r_f}^2, \ \ H_{0P} = -\frac{1}{2a}\nabla_{s_1}^2 - \frac{1}{2a}\nabla_{s_2}^2 \\
a = \frac{M_P}{M_P + 1}, \ \ b = \frac{M_T}{M_T + 1}
\end{aligned}\right\} . \quad (4)$$

Herein, the limits $1/M_{T,P} \ll 1$ are exploited to neglect the mass-polarization potential operators $-(1/M_T)\nabla_{x_1} \cdot \nabla_{x_2}$ in $H_{0T}$ and $-(1/M_P)\nabla_{s_1} \cdot \nabla_{s_2}$ in $H_{0P}$. Thus, the total interactive Hamiltonian $H$ can also be cast into the two forms connected with the initial/final Hamiltonians $H_{i,f}$:

$$\left.\begin{aligned}
H = H_0 + V = H_i + V_i = H_f + V_f \\
H_i = H_0 + V_T = K_i + h_i, \ \ h_i = H_{0T} + V_T \\
H_f = H_0 + V_P = K_f + h_f, \ \ h_f = H_{0P} + V_P
\end{aligned}\right\} , \quad (5)$$

where $V$ is the complete interaction and $h_{i,f}$ are the purely electronic Hamiltonians. Further, $V_{i,f}$ are the initial/final perturbation interactions, whereas $V_T$ and $V_P$ are the potentials in the bound systems $(Z_T; e_1, e_2)_i$ and $(Z_P; e_1, e_2)_f$, respectively:

$$\left.\begin{aligned}
V = V_{PT} + V_{12} + (V_{P1} + V_{P2}) + (V_{T1} + V_{T2}) \\
V_{PT} = \frac{Z_P Z_T}{R}, \ \ V_{12} = \frac{1}{r_{12}} \\
V_P = V_{P1} + V_{P2} + V_{12}, \ \ V_T = V_{T1} + V_{T2} + V_{12} \\
V_{Pk} = -\frac{Z_P}{s_k}, \ \ V_{Tk} = -\frac{Z_T}{x_k} \ \ (k = 1, 2)
\end{aligned}\right\} . \quad (6)$$

Asymptotically, i.e. at large inter-particle distances $(R \to \infty)$, the perturbations $V_{i,f}$ are of long range:

$$\left.\begin{aligned}
V_i \approx V_i^\infty \ (R \to \infty), \ \ V_i^\infty = \frac{Z_P(Z_T - 2)}{R} \\
V_f \approx V_f^\infty \ (R \to \infty), \ \ V_f^\infty = \frac{Z_T(Z_P - 2)}{R}
\end{aligned}\right\} . \quad (7)$$

Therefore, except for the special cases $Z_{T,P} = 2$, the interactions $V_{i,f}$ are respectively reduced to the non-zero Coulombic potential $V_{i,f}^\infty$ in the asymptotic scattering region $(R \to \infty)$.

The unperturbed initial/final states $\Phi_{i,f}$ are the solutions of their channel Hamiltonians $H_{i,f}$:

$$
\left.
\begin{aligned}
(H_i - E_i)\Phi_i = 0, \quad E_i = \frac{k_i^2}{2\mu_i} + \varepsilon_i^{\mathrm{T}} \\
(H_f - E_f)\Phi_f = 0, \quad E_f = \frac{k_f^2}{2\mu_f} + \varepsilon_f^{\mathrm{P}} \\
E_i = E_f = E
\end{aligned}
\right\}. \tag{8}
$$

In the total energies $E_{i,f}$ of the entire system, $k_{i,f}^2/(2\mu_{i,f})$ and $\varepsilon_{i,f}^{\mathrm{T,P}}$ are the kinetic energies of the heavy scattering aggregates and the electronic binding energies in the entrance/exit channels, respectively. The eigen-energies $\varepsilon_{i,f}^{\mathrm{T,P}}$ and the corresponding eigen-functions $\varphi_{i,f}$ are the solutions of their eigen-value problems:

$$
(h_i - \varepsilon_i^{\mathrm{T}})\varphi_i(\boldsymbol{x}_1, \boldsymbol{x}_2) = 0, \quad (h_f - \varepsilon_f^{\mathrm{P}})\varphi_f(\boldsymbol{s}_1, \boldsymbol{s}_2) = 0. \tag{9}
$$

Using these eigen-problems, the solutions of the equations from (8) for $\Phi_{i,f}$ read as:

$$
\Phi_i = \varphi_i(\boldsymbol{x}_1, \boldsymbol{x}_2)e^{i\boldsymbol{k}_i \cdot \boldsymbol{r}_i}, \quad \Phi_f = \varphi_f(\boldsymbol{s}_1, \boldsymbol{s}_2)e^{-i\boldsymbol{k}_f \cdot \boldsymbol{r}_f}, \tag{10}
$$

where $e^{\pm i\boldsymbol{k}_{i,f} \cdot \boldsymbol{r}_{i,f}}$ are the plane waves for the free relative motions of heavy scattering aggregates. Note that the minus sign in the exponent $e^{-i\boldsymbol{k}_f \cdot \boldsymbol{r}_f}$ is due to the mentioned definition of $\boldsymbol{k}_f$ as the momentum vector of $(Z_{\mathrm{P}}; e_1, e_2)_f$ relative to T rather than the other way around.

In calculations for heavy particle collisions, it is convenient to exploit the following amply justified approximations:

$$
\boldsymbol{R} \approx \boldsymbol{r}_i, \quad \boldsymbol{R} \approx -\boldsymbol{r}_f \quad (M_{\mathrm{P,T}} \gg 1). \tag{11}
$$

This can be utilized in the potential $V_{\mathrm{PT}}$, $V_{i,f}$, $V_{i,f}^{\infty}$ and their Coulomb continuum wave functions (or the associated asymptotes) for the relative motions of heavy particles, e.g:

$$
V_i^{\infty} \approx \frac{Z_{\mathrm{P}}(Z_{\mathrm{T}} - 2)}{r_i}, \quad V_f^{\infty} \approx \frac{Z_{\mathrm{T}}(Z_{\mathrm{P}} - 2)}{r_f} \quad (M_{\mathrm{P,T}} \gg 1). \tag{12}
$$

However, for the rearrangement processes of type (1), it is not allowed to apply (11) to the initial/final unperturbed states $\Phi_{i,f}$ nor to their product:

$$
\Phi_i \Phi_f^{\star} = \varphi_i \varphi_f^{\star} e^{i\boldsymbol{k}_i \cdot \boldsymbol{r}_i + i\boldsymbol{k}_f \cdot \boldsymbol{r}_f}. \tag{13}
$$

The reason is that the usage of the approximations (11) in (13) for $\Phi_{i,f}$ or $\Phi_i \Phi_f^{\star}$ would obliterate the ETFs whose importance grows with augmenting impact energy. For the two electrons in double charge exchange, the ETFs are $-i\boldsymbol{v} \cdot (\boldsymbol{x}_1 + \boldsymbol{x}_2)$.

The channel states $\Phi_{i,f}$ persist to be unperturbed only if the short-range potentials remain in the asymptotic region of scattering. However, for $Z_{T,P} \neq 2$ in process (1), the long-range Coulomb potentials $V_{i,f}^\infty$ persist at $R \to \infty$. In other words, the scattering particles are not asymptotically free because they move in the Coulomb fields $V_{i,f}^\infty$. Such motions cannot be described by the plane waves $e^{\pm i k_{i,f} \cdot r_{i,f}}$ since $V_{i,f}^\infty(R)$ generate Coulomb distortions even at $R \to \infty$. Thus, for $Z_{T,P} \neq 2$ in process (1), the relative motions of the heavy scattering aggregates should be described by the full Coulomb wave functions for $V_{i,f}^\infty(R)$. At large distances, the leading term of the asymptotic behavior of any given Coulomb continuum wave function is represented by the Coulomb logarithmic phase factor (the eikonal phase).

To accommodate for these special features of Coulomb scattering, the unperturbed channel states $\Phi_{i,f}$ should be "dressed" through the appropriate modifications of their phases. The presence of the long-range Coulomb potentials at $R \to \infty$, dictates that the phase adjustments of the unperturbed channel states are to be made via multiplications of $\Phi_{i,f}$ by the Coulomb asymptotic states $\mathcal{E}_{i,f}^\pm$ for $V_{i,f}^\infty$ from (7) or (12):

$$\left.\begin{array}{c} \mathcal{E} = e^{\pm i v_{i,f} \ln(k_{i,f} r_{i,f} - k_{i,f} \cdot r_{i,f})} \approx e^{\pm i v_{i,f} \ln(k_{i,f} R \mp k_{i,f} \cdot R)} \\[2mm] v_i = \dfrac{Z_P(Z_T - 2)}{v}, \quad v_f = \dfrac{Z_T(Z_P - 2)}{v} \end{array}\right\}. \tag{14}$$

The Coulomb-dressed channel states $\Phi_{i,f}^\pm$ can now be introduced by means of the products:

$$\left.\begin{array}{c} \Phi_{i,f}^\pm = \Phi_{i,f} \mathcal{E}_{i,f}^\pm \\[1mm] \Phi_{i,f}^\pm = \Phi_{i,f} e^{\pm i v_{i,f} \ln(k_{i,f} r_{i,f} - k_{i,f} \cdot r_{i,f})} \\[1mm] \Phi_{i,f}^\pm = \varphi_{i,f} e^{\pm i k_{i,f} \cdot r_{i,f} \pm i v_{i,f} \ln(k_{i,f} r_{i,f} - k_{i,f} \cdot r_{i,f})} \end{array}\right\}. \tag{15}$$

For consistency, it is not permitted to modify the scattering wave functions without the appropriate alterations of the associated perturbation potentials. The unperturbed channel states $\Phi_{i,f}$ must correspond to the channel perturbations $V_{i,f}$. Therefore, if $\Phi_{i,f}$ are changed to $\Phi_{i,f}^\pm$, the associated perturbation potentials $V_{i,f}$ must be altered accordingly. In order to make the sought phase corrections to $\Phi_{i,f}$, the Coulomb potentials $V_{i,f}^\infty$ should be subtracted from $V_{i,f}$ to yield the modified interactions $\widetilde{V}_{i,f}$ of short range at $R \to \infty$:

$$\left.\begin{array}{c} \widetilde{V}_i \equiv V_i - V_i^\infty = \dfrac{2Z_P}{R} - \dfrac{Z_P}{s_1} - \dfrac{Z_P}{s_2} \\[3mm] \widetilde{V}_f \equiv V_f - V_f^\infty = \dfrac{2Z_T}{R} - \dfrac{Z_T}{x_1} - \dfrac{Z_T}{x_2} \end{array}\right\}. \tag{16}$$

Hence, it is $\Phi_{i,f}^\pm$ and $\widetilde{V}_{i,f}$ that should be coupled together in the Coulomb-modified entrance/exit channels. Working with the modified channel states $\Phi_{i,f}^\pm$ [11] is formally equivalent to dealing with the Coulomb-distorted Møller wave operators [9]. In practice, the former is more manageable than the latter.

The quantum-mechanical dynamics of the four-body problem in process (1) is described by the complete Schrödinger equation for the full wave function $\Psi$. This latter wave function has the variants $\Psi_i^+$ and $\Psi_f^-$ with the outgoing and incoming boundary conditions for the initial and final states, consistent with $\Phi_i^+$ and $\Phi_f^-$ at $R \to \infty$, in the entrance and exit channels, respectively:

$$\left. \begin{array}{c} (H - E)\Psi = 0, \ (H - E_{i,f})\Psi_{i,f}^{\pm} = 0 \\ \Psi_{i,f}^{\pm} \approx \Phi_{i,f}^{\pm} \ \ (R \to \infty) \end{array} \right\}. \tag{17}$$

This means that the complete Schrödinger equations for the initial/final total scattering states should be solved with the physical boundary conditions requiring that $\Psi_{i,f}^{\pm}$ coincide asymptotically with the Coulomb-dressed channel states $\Phi_{i,f}^{\pm}$.

If the perturbation potentials $V_{i,f}$ were of short range, the exact prior/post transition amplitudes $T_{if}^{\mp}$ would be defined as:

$$T_{if}^- = \langle \Psi_f^- | V_i | \Phi_i \rangle, \ \ T_{if}^+ = \langle \Phi_f \left| V_f^{\dagger} \right| \Psi_i^+ \rangle. \tag{18}$$

This definition should be modified when $V_{i,f}$ are of long range because of their non-vanishing Coulombic tails $V_{i,f}^{\infty} \neq 0$ at $R \to \infty$. In such cases, $\Phi_{i,f}$ from (10) do not possess the correct asymptotic forms. As stated, the proper modifications consist of replacing $\Phi_{i,f}$ by $\Phi_{i,f}^{\pm}$ and by simultaneously subtracting $V_{i,f}^{\infty}$ from $V_{i,f}$. Such a twofold change maps $T_{if}^{\mp}$ from (18) to:

$$T_{if}^- = \langle \Psi_f^- \left| \widetilde{V}_i \right| \Phi_i^+ \rangle, \ \ T_{if}^+ = \langle \Phi_f^- \left| \widetilde{V}_f^{\dagger} \right| \Psi_i^+ \rangle, \tag{19}$$

where $\widetilde{V}_{i,f}$ are from (16). For determination of the initial/final total scattering states $\Psi_{i,f}^{\pm}$ for process (1), the distorted wave theory offers a flexible framework. This can be used to obtain the transition amplitudes containing the total scattering wave functions of the correct asymptotic behaviors consistent with the corresponding perturbation potentials. To proceed within this formalism, the distorted waves $\chi_{i,f}^{\pm}$, with the same exact asymptotic behaviors as for $\Psi_{i,f}^{\pm}$ at $R \to \infty$, are defined by the following equations:

$$\left. \begin{array}{c} \left( H_{i,f} + W_{i,f} - E \right) \chi_{i,f}^{\pm} = 0 \\ \chi_{i,f}^{\pm} \approx \Phi_{i,f}^{\pm} \ (R \to \infty) \end{array} \right\}. \tag{20}$$

Here, $W_{i,f}$ are some distorting potentials of the type $W_{i,f} = w_{i,f} + W_{i,f}^{\mathrm{d}}$, with short-range and long-range interactions $w_{i,f}$ and $W_{i,f}^{\mathrm{d}}$, respectively.

Thus, the original problems in (17), having the solutions $\Psi_{i,f}^{\pm}$ without the distorted wave formalism, are represented by the model problems in (20) whose solutions $\chi_{i,f}^{\pm}$ are in the distorted wave representation. However, it is necessary to connect the original and model problems. To that end, the Schrödinger operator $E - H$ from (17) should

appear also in (20). Inserting $H_{i,f} = H - V_{i,f}$ into (20), the ensuing equations $(H - E)\chi_{i,f}^{\pm} = (V_{i,f} - W_{i,f})\chi_{i,f}^{\pm}$ are combined with (17) to have:

$$\left.\begin{array}{c} (H - E)\chi_{i,f}^{\pm} = U_{i,f}\chi_{i,f}^{\pm} \\ (H - E)\Psi_{i,f}^{\pm} = 0 \end{array}\right\}, \tag{21}$$

$$U_{i,f} = V_{i,f} - W_{i,f}. \tag{22}$$

Similarly to the exact Schrödinger equations, the distorted wave equations now contain the operator $H - E$ but, additionally, they have the extra terms $U_{i,f}\chi_{i,f}^{\pm}$. As they stand, the wave functions $\chi_{i,f}^{\pm}$ and $\Psi_{i,f}^{\pm}$ remain decoupled. They can be coupled by subtracting the second from the first equations in (21) so that:

$$(H - E)\chi_{i,f}^{\pm} - (H - E)\Psi_{i,f}^{\pm} = U_{i,f}\chi_{i,f}^{\pm}, \tag{23}$$

or equivalently

$$(E - H)(\Psi_{i,f}^{\pm} - \chi_{i,f}^{\pm}) = U_{i,f}\chi_{i,f}^{\pm}. \tag{24}$$

If the inverse of the operator $E - H$ were non-singular, we could multiply (24) from left by $(E - H)^{-1}$ to deduce the difference $\Psi_{i,f}^{\pm} - \chi_{i,f}^{\pm}$. However, $(E - H)^{-1}$ has singularities at the eigen-values of $H$. Nevertheless, these singularities, as the real-valued eigen-energies ($H$ is a Hermitean operator), can be avoided by adding the purely imaginary terms $\pm i\epsilon$ to $E - H$ in (24), where $\epsilon$ is an infinitesimally small positive number, which tends to zero through positive numbers:

$$(E - H \pm i\epsilon)(\Psi_{i,f}^{\pm} - \chi_{i,f}^{\pm}) = U_{i,f}\chi_{i,f}^{\pm}, \tag{25}$$

provided that

$$i\epsilon(\Psi_{i,f}^{\pm} - \chi_{i,f}^{\pm}) = 0 \quad \text{at } \epsilon \to 0^+. \tag{26}$$

Thus, the inverses $(E - H \pm i\epsilon)^{-1}$ of $E - H \pm i\epsilon$ are non-singular for $\epsilon > 0$. Therefore, it is now allowed to multiply (25) from left by $(E - H \pm i\epsilon)^{-1}$. Subsequently, the usage of the relations $(E - H \pm i\epsilon)^{-1}(E - H \pm i\epsilon) = 1$ yields:

$$\Psi_{i,f}^{\pm} = \left(1 + \frac{1}{E - H \pm i\epsilon}U_{i,f}\right)\chi_{i,f}^{\pm}, \; \epsilon \to 0^+. \tag{27}$$

These equations can be written more compactly when the operators $1/(E - H \pm i\epsilon)$ are denoted by $G^{\pm}$:

$$\Psi_{i,f}^{\pm} = \left(1 + G^{\pm}U_{i,f}\right)\chi_{i,f}^{\pm}, \tag{28}$$

$$G^{\pm}(E) = \frac{1}{E - H \pm i\epsilon}, \quad \epsilon \to 0^+. \tag{29}$$

Operators $G^{\pm}(E)$ represent the resolvents, recognized as the standard full Green's operators. In the customary theory of scattering, the Green operators $G^{\pm}(E)$ are first defined as the two equivalent resolvents of $E - H$ and subsequently related to $\Psi_{i,f}^{\pm}$. Alternatively, to arrive at (28), the expressions for $G^{\pm}(E)$ in (29) are derived in the just outlined steps. This came out naturally from connecting the exact Schrödinger Eq. (17) for $\Psi_{i,f}^{\pm}$ to the distorted wave Eq. (20) for $\chi_{i,f}^{\pm}$.

In the distorted wave formalism, the exact transition amplitudes with the prior and post interactions are given by:

$$T_{if}^{-} = \langle \Psi_f^{-} | U_i | \chi_i^{+} \rangle, \ \ T_{if}^{+} = \langle \chi_f^{-} | U_f^{\dagger} | \Psi_i^{+} \rangle. \tag{30}$$

It is very important to draw attention to a parallel structure of (19) and (30). These two transition amplitudes share the same exact wave functions $\Psi_{i,f}^{\pm}$. Therein, the scattering states $\Phi_{i,f}^{\pm}$ and $\chi_{i,f}^{\pm}$ are both associated with the same channel potentials $V_{i,f}$ from which, however, two different interaction pairs $V_{i,f}^{\infty}$ and $W_{i,f}$ are subtracted. This secures the emphasized crucial consistency between the scattering states and the corresponding perturbation potentials that produce the transitions.

If the terms $G^{\pm}U_{i,f}$ are neglected in (28), the lowest-order approximations to $\Psi_{i,f}^{\pm}$ in the distorted wave formalism would emerge as:

$$\Psi_{i,f}^{\pm} \approx \chi_{i,f}^{\pm}. \tag{31}$$

In such a case, the lowest-order transition amplitudes (also denoted by $T_{if}^{\mp}$) are:

$$T_{if}^{-} = \langle \chi_f^{-} | U_i | \chi_i^{+} \rangle, \ \ T_{if}^{+} = \langle \chi_f^{-} | U_f^{\dagger} | \chi_i^{+} \rangle. \tag{32}$$

From here, various theories can be formulated for different sets of the distorted wave functions and distorting potentials. One of such theories is the SDS-4B method [4, 5].

## 2.2 Four-body single-double scattering method: SDS-4B

### 2.2.1 Description of the entrance channel

In the entrance channel, we look for the initial distorted wave $\chi_i^{+}$ as a factorized function:

$$\chi_i^{+} = \varphi_i(\boldsymbol{x}_1, \boldsymbol{x}_2)\zeta_i^{+}, \tag{33}$$

where $\zeta_i^{+}$ is to be found. This product should reflect the influence of the field from the external perturbation (caused by the presence of the projectile) to the initial channel state $\Phi_i$ from (10). To proceed, the long-range perturbation interaction potential $V_i$ from (5) is partitioned as:

$$V_i = \frac{Z_P Z_T}{R} - \frac{Z_P}{s_1} - \frac{Z_P}{s_2} = \left[ \frac{Z_P(Z_T - 1)}{R} - \frac{Z_P}{s_1} \right] + \left( \frac{Z_P}{R} - \frac{Z_P}{s_2} \right). \qquad (34)$$

This subdivision of $V_i$ is made to group $Z_P(Z_T - 1)/R - Z_P/s_1$ with $H_0$ and $Z_P/R - Z_P/s_2$ with $U_i$. At $R \to \infty$, the potential $Z_P/R - Z_P/s_2$ is of short range since it decreases as $1/R^n$ ($n > 1$). In the same limit $R \to \infty$, the interaction $Z_P(Z_T - 1)/R - Z_P/s_1$ is of long range since it behaves like $Z_P(Z_T - 2)/R \approx Z_P(Z_T - 2)/r_i \equiv V_i^\infty$ on account of (7) and (12).

By inserting (33) into Eq. (20) for $\chi_i^+$ and using the eigen-value problem (9) for $\varphi_i$, it follows:

$$\varphi_i \left[ \Delta E_i - H_0 - \frac{Z_P(Z_T - 1)}{R} + \frac{Z_P}{s_1} \right] \zeta_i^+$$
$$+ \left[ U_i - Z_P \left( \frac{1}{R} - \frac{1}{s_2} \right) \right] \chi_i^+ + \frac{1}{b} \sum_{k=1}^{2} \nabla_{x_k} \varphi_i \cdot \nabla_{x_k} \zeta_i^+ = 0, \qquad (35)$$

where $\Delta E_i = E - \varepsilon_i^T = k_i^2/(2\mu_i)$. In (35), the potential $U_i$ is now chosen according to:

$$U_i \chi_i^+ = Z_P \left( \frac{1}{R} - \frac{1}{s_2} \right) \chi_i^+ - \frac{1}{b} \sum_{k=1}^{2} \nabla_{x_k} \varphi_i \cdot \nabla_{x_k} \zeta_i^+. \qquad (36)$$

This selection of $U_i$ reduces the inhomogeneous Eq. (35) for $\zeta_i^+$ to its homogeneous counterpart:

$$\left[ H_0 + \frac{Z_P(Z_T - 1)}{R} - \frac{Z_P}{s_1} - \Delta E_i \right] \zeta_i^+ = 0. \qquad (37)$$

In (37), the independent variables can be separated in the heavy-particle mass limit. Then, with the help of the approximations from (11), the exact solution of (37) is obtained as:

$$\zeta_i^+ = \mu_i^{-i v_P} \mathcal{N}^+(\tilde{v}_i) \, e^{i k_i \cdot r_i} \mathcal{D}_i^+(s_1) {}_1F_1(-i \tilde{v}_i, 1, i k_i r_f + i k_i \cdot r_f), \qquad (38)$$

$$\mathcal{D}_i^+(s_1) = N^+(v_P) {}_1F_1(i v_P, 1, i v s_1 + i \boldsymbol{v} \cdot \boldsymbol{s}_1), \qquad (39)$$

$$\mathcal{N}^+(\tilde{v}_i) = \Gamma(1 + i \tilde{v}_i) e^{-\pi \tilde{v}_i/2}, \quad \tilde{v}_i = \frac{Z_P(Z_T - 1)}{v}, \qquad (40)$$

$$N^+(v_P) = \Gamma(1 - i v_P) e^{\pi v_P/2}, \quad v_P = \frac{Z_P}{v}. \qquad (41)$$

Here, $\Gamma$ is the complex Euler gamma function and ${}_1F_1$ is the Gauss confluent hypergeometric function (the Kummer hypergeometric function). By design, the expression (38) for $\zeta_i^+$ does not depend of the coordinates of electron $e_2$. This leads to the relation $\nabla_{x_2} \zeta_i^+ = 0$, which annuls the term $k = 2$ from the sum over $k$ on the rhs of Eq. (36),

so that:

$$U_i \chi_i^+ = Z_P \left( \frac{1}{R} - \frac{1}{s_2} \right) \chi_i^+ - \frac{1}{b} \boldsymbol{\nabla}_{x_1} \varphi_i \cdot \boldsymbol{\nabla}_{x_1} \zeta_i^+. \tag{42}$$

Substitution of $\zeta_i^+$ from (38) into (33) gives the distorted wave $\chi_i^+$:

$$\begin{aligned}
\chi_i^+ = {} & \mu_i^{-i v_P} \mathcal{N}^+(\tilde{v}_i) N^+(v_P) e^{i\boldsymbol{k}_i \cdot \boldsymbol{r}_i} \varphi_i(\boldsymbol{x}_1, \boldsymbol{x}_2) \\
& \times {}_1F_1(-i\tilde{v}_i, 1, i k_i r_f + i\boldsymbol{k}_i \cdot \boldsymbol{r}_f) {}_1F_1(i v_P, 1, i v s_1 + i\boldsymbol{v} \cdot \boldsymbol{s}_1).
\end{aligned} \tag{43}$$

In the mass limit, this solution satisfies the correct asymptotic behavior $\chi_i^+ \approx \Phi_i^+ (R \to \infty)$ prescribed by (20) for $\chi_i^+$. This can be readily verified by using the standard asymptotic forms of the two confluent hypergeometric functions from (43). Such a key feature follows from the mentioned long-range asymptote $V_i^\infty$ of the perturbation potential $Z_P(Z_T - 1)/R - Z_P/s_1$ from Eq. (37) for $\zeta_i^+$. The performed analysis completes the description the entrance channel in the SDS-4B method through specifying the perturbation potential operator $U_i$ and the initial distorted wave $\chi_i^+$ in (42) and (43), respectively.

### 2.2.2 Description of the exit channel

Similarly to the preceding briefing, the distorted wave $\chi_f^-$ in the exit channel is also factorized in an analogous way:

$$\chi_f^- = \varphi_f(\boldsymbol{s}_1, \boldsymbol{s}_2) \zeta_f^-. \tag{44}$$

The task is then to determine the unknown function $\zeta_f^-$. To start, the perturbation potential $V_f$ is reshuffled first as:

$$V_f = \frac{Z_P Z_T}{R} - \frac{Z_T}{x_1} - \frac{Z_T}{x_2} = \left[ \frac{Z_T(Z_P - 1)}{R} - \frac{Z_T}{x_1} \right] + \left( \frac{Z_T}{R} - \frac{Z_T}{x_2} \right). \tag{45}$$

With such a splitting of $V_f$, the potential $Z_T(Z_P - 1)/R - Z_T/x_1$ is associated with $H_0$ and $Z_T/R - Z_T/x_2$ with $U_f$. At $R \to \infty$, the interaction $Z_T/R - Z_T/x_2$ is of short range, whereas the potential $Z_T(Z_P - 1)/R - Z_T/x_1$ becomes Coulombic, after using (7) and (12), i.e. $Z_T(Z_P - 2)/R \approx Z_T(Z_P - 2)/r_f \equiv V_f^\infty$.

By substituting (44) into (20) for $\chi_f^-$ and employing the eigen-value problem (9) for $\varphi_f$, we have:

$$\begin{aligned}
& \varphi_f \left[ \Delta E_f - H_0 - \frac{Z_T(Z_P - 1)}{R} + \frac{Z_T}{x_1} \right] \zeta_f^- \\
& + \left[ U_f - Z_T \left( \frac{1}{R} - \frac{1}{x_2} \right) \right] \chi_f^- + \frac{1}{a} \sum_{k=1}^{2} \boldsymbol{\nabla}_{s_k} \varphi_f \cdot \boldsymbol{\nabla}_{s_k} \zeta_f^- = 0, \tag{46}
\end{aligned}$$

where $\Delta E_f = E - \varepsilon_f^P = k_f^2/(2\mu_f)$. Here, the potential $U_f$ is selected as:

$$U_f \chi_f^- = Z_T \left( \frac{1}{R} - \frac{1}{x_2} \right) \chi_f^- - \frac{1}{a} \sum_{k=1}^2 \nabla_{s_k} \varphi_f \cdot \nabla_{s_k} \zeta_f^-. \tag{47}$$

This transforms the inhomogeneous Eq. (46) to its homogeneous companion:

$$\left[ H_0 + \frac{Z_T(Z_P - 1)}{R} - \frac{Z_T}{x_1} - \Delta E_f \right] \zeta_f^- = 0. \tag{48}$$

Exploiting again the mass limit for heavy particles, the approximation $\boldsymbol{R} \approx -\boldsymbol{r}_f$ from (11) can be employed to make Eq. (48) separable. Due to this circumstance, the solution of Eq. (48) for $\zeta_f^-$ is obtained by a standard procedure [4] as:

$$\zeta_f^- = \mu_f^{i\nu_T} \mathcal{N}^-(\tilde{\nu}_f) e^{-i\boldsymbol{k}_f \cdot \boldsymbol{r}_f} \mathcal{D}_f^-(\boldsymbol{x}_1)\, {}_1F_1(i\tilde{\nu}_f, 1, -ik_f r_i - i\boldsymbol{k}_f \cdot \boldsymbol{r}_i), \tag{49}$$

$$\mathcal{D}_f^-(\boldsymbol{x}_1) = N^-(\nu_T)\, {}_1F_1(-i\nu_T, 1, -ivx_1 - i\boldsymbol{v} \cdot \boldsymbol{x}_1), \tag{50}$$

$$\mathcal{N}^-(\tilde{\nu}_f) = \Gamma(1 - i\tilde{\nu}_f) e^{-\pi \tilde{\nu}_f/2}, \quad \tilde{\nu}_f = \frac{Z_T(Z_P - 1)}{v}, \tag{51}$$

$$N^-(\nu_T) = \Gamma(1 + i\nu_T) e^{\pi \nu_T/2}, \quad \nu_T = \frac{Z_T}{v}. \tag{52}$$

By construction, the function (49) is independent of the coordinates of electron $e_2$, so that $\nabla_{s_2} \zeta_f^- = 0$. This makes the term $k = 2$ in the sum over $k$ on the rhs of Eq. (47) disappear and the expression for $U_f$ is reduced to:

$$U_f \chi_f^- = Z_T \left( \frac{1}{R} - \frac{1}{x_2} \right) \chi_f^- - \frac{1}{a} \nabla_{s_1} \varphi_f \cdot \nabla_{s_1} \zeta_f^-. \tag{53}$$

Insertion of $\zeta_f^-$ from (49) into (44) specifies the distorted wave $\chi_f^-$ as:

$$\chi_f^- = \mu_f^{i\nu_T} \mathcal{N}^-(\tilde{\nu}_f) N^-(\nu_T) e^{-i\boldsymbol{k}_f \cdot \boldsymbol{r}_f} \varphi_f(\boldsymbol{s}_1, \boldsymbol{s}_2)$$
$$\times\, {}_1F_1(i\tilde{\nu}_f, 1, -ik_f r_i - i\boldsymbol{k}_f \cdot \boldsymbol{r}_i)\, {}_1F_1(-i\nu_T, 1, -ivx_1 - i\boldsymbol{v} \cdot \boldsymbol{x}_1). \tag{54}$$

This function possesses the proper asymptotic behavior stated in (20) for $\chi_f^-$. To check it in the mass limit, it suffices to use the asymptotic forms of the confluent hypergeometric functions from (54). In fact, already the partitioning of $V_f$ in (45) gives a hint that at $R \to \infty$ the long-range Coulomb tail $Z_T(Z_P - 2)/R = V_f^\infty$ of potential $Z_T(Z_P - 1)/R - Z_T/x_1$ will produce the asymptotically correct $\zeta_f^-$. This latter function then provides the distorted wave $\chi_f^-$ with the requested behavior $\chi_f^- \approx \Phi_f^-$ at $R \to \infty$.

By completing this description of the exit channel, we can conclude that the pairs of the dynamic quantities $\{\chi_i^+, U_i\}$ and $\{\chi_f^-, U_f\}$ in the SDS-4B method are fully specified in accordance with the correct initial and final boundary conditions. If desired,

$U_{i,f}$ can be extracted as the operator perturbation potentials from $U_{i,f}\chi_{i,f}^{\pm}$ in (42) and (53). However, this is unnecessary since it is the quantities $U_{i,f}\chi_{i,f}^{\pm}$ that appear in the transition amplitudes $T_{if}^{\mp}$ in (30).

In setting up the pairs $\{\chi_{i,f}^{\pm}, U_{i,f}\}$, the pertinent bound-state eigen-value problems in (9) are used. In practice, however, the existing approximations to the wave functions $\varphi_{i,f}$ do not satisfy exactly their respective eigen-equations from (9) for any helium-like atomic systems. Therefore, in principle, the terms $(h_{i,f} - \varepsilon_{i,f}^{\mathrm{T,P}})\varphi_{i,f} \neq 0$ should be kept in the equations for $\chi_{i,f}^{\pm}$, respectively. This would modify $U_{i,f}\chi_{i,f}^{\pm}$ by subtracting the non-zero terms $-\zeta_{i,f}^{\pm}(h_{i,f} - \varepsilon_{i,f}^{\mathrm{T,P}})\varphi_{i,f}$ from the right hand sides of Eqs. (36) and (47), respectively.

However, the explicit contributions of these additional terms have been found to be completely insignificant in computations on total cross sections $Q$ within the CB1-4B method for double charge exchange in the $\mathrm{He}^{2+} - \mathrm{He}$ collisions [21]. It is reasonable to suppose that this conclusion could also be valid for the SDS-4B method. Under this assumption, we opted not to include the supplementary perturbative terms $-\zeta_{i,f}^{\pm}(h_{i,f} - \varepsilon_{i,f}^{\mathrm{T,P}})\varphi_{i,f}$ in $U_{i,f}\chi_{i,f}^{\pm}$, respectively.

### 2.2.3 Transition amplitudes

Having determined $\{\chi_{i,f}^{\pm}, U_{i,f}\}$, we can now return to (32) for prior $T_{if}^{-}$ and post $T_{if}^{+}$ transition amplitudes. To point to the SDS-4B method, these amplitudes are denoted by $T_{if}^{(\mathrm{SDS-4B})\mp}$ and we can write their symmetrized forms as:

$$
\begin{aligned}
T_{if}^{(\mathrm{SDS-4B})-}(\boldsymbol{\eta}) = \iiint \mathrm{d}\boldsymbol{r}_i \mathrm{d}\boldsymbol{x}_1 \mathrm{d}\boldsymbol{x}_2 \mathcal{P}_{12}\chi_f^{-\star} \\
\times \left[ Z_{\mathrm{P}}\left(\frac{1}{R} - \frac{1}{s_2}\right)\chi_i^{+} - \frac{1}{b}\boldsymbol{\nabla}_{x_1}\varphi_i \cdot \boldsymbol{\nabla}_{s_1}\zeta_i^{+} \right],
\end{aligned} \tag{55}
$$

$$
\begin{aligned}
T_{if}^{(\mathrm{SDS-4B})+}(\boldsymbol{\eta}) = \iiint \mathrm{d}\boldsymbol{r}_f \mathrm{d}\boldsymbol{s}_1 \mathrm{d}\boldsymbol{s}_2 \mathcal{P}_{12}\chi_i^{+} \\
\times \left[ Z_{\mathrm{T}}\left(\frac{1}{R} - \frac{1}{x_2}\right)\chi_f^{-\star} - \frac{1}{a}\boldsymbol{\nabla}_{s_1}\varphi_f^{\star} \cdot \boldsymbol{\nabla}_{x_1}\zeta_f^{-\star} \right],
\end{aligned} \tag{56}
$$

$$
\mathcal{P}_{12} = \frac{1 + P_{12}}{\sqrt{2}}. \tag{57}
$$

Here, the mass constants $a$ and $b$, multiplying the gradient operators, are formally kept, but they can be set to unity in the heavy particle mass unit. This would be consistent given that the same mass limit $1/M_{\mathrm{P,T}} \ll 1$ was also used in deriving the main quantities $\{\chi_{i,f}^{\pm}, U_{i,f}\}$ in the SDS-4B method.

In (57), quantity $P_{12}$ is the permutation operator, which exchanges the role of electrons $e_{1,2}$. Without the symmetrization operator $\mathcal{P}_{12}$, the unsymmetrized transition amplitudes from (55) and (56) describe electrons $e_1$ and $e_2$ as undergoing the single- and double-scatterings, respectively. The factor $\mathcal{P}_{12}$ symmetrizes these transition amplitudes to account for the fact that the same probability is obtained when electrons $e_1$ and $e_2$ undergo the double- and single-scatterings, respectively.

In the matrix elements (55) and (56) within the usual eikonal setting, the product of the two Kummer functions for the relative motion of heavy nuclei can be simplified in the usual way [4]:

$$\mathcal{N}^+(\tilde{v}_i)\mathcal{N}^{-\star}(\tilde{v}_f)\,_1F_1(-i\tilde{v}_i, 1, ik_i r_f + i\boldsymbol{k}_i \cdot \boldsymbol{r}_f)\,_1F_1(-i\tilde{v}_f, 1, ik_f r_i + \boldsymbol{k}_f \cdot \boldsymbol{r}_i)$$

$$= e^{i\tilde{v}_i \ln \mu(vR - \boldsymbol{v}\cdot\boldsymbol{R})} e^{i\tilde{v}_f \ln \mu(vR + \boldsymbol{v}\cdot\boldsymbol{R})}$$

$$= (\mu v\rho)^{2i\tilde{v}_i}(vR + \boldsymbol{v} \cdot \boldsymbol{R})^{-i\xi} = (\mu v\rho)^{2i\tilde{v}_f}(vR - \boldsymbol{v} \cdot \boldsymbol{R})^{i\xi}, \tag{58}$$

$$\xi = \frac{Z_{\mathrm{T}} - Z_{\mathrm{P}}}{v}, \quad \mu = \frac{M_{\mathrm{P}} M_{\mathrm{T}}}{M_{\mathrm{P}} + M_{\mathrm{T}}}, \tag{59}$$

where $(\mu vR + \mu\boldsymbol{v}\cdot\boldsymbol{R})(\mu vR - \mu\boldsymbol{v}\cdot\boldsymbol{R}) = (\mu v\rho)^2$ due to $\boldsymbol{R} = \boldsymbol{\rho} + v\hat{\boldsymbol{Z}}$ and $\boldsymbol{\rho}\cdot\boldsymbol{v} = 0$.

### 2.2.4 Cross sections

Of course, the constant phases of unit amplitudes $(\mu v)^{2i\tilde{v}_{f,i}}$ from (58) disappear from differential and total cross sections $(\mathrm{d}/\mathrm{d}\Omega)Q_{if}^{(\mathrm{SDS}-4\mathrm{B})\mp}$ and $Q_{if}^{(\mathrm{SDS}-4\mathrm{B})\mp}$, respectively. However, the phases $\rho^{2i\tilde{v}_{f,i}}$ from (58) need to be kept in $(\mathrm{d}/\mathrm{d}\Omega)Q_{if}^{(\mathrm{SDS}-4\mathrm{B})\mp}$, but not in $Q_{if}^{(\mathrm{SDS}-4\mathrm{B})\mp}$ to which they give no contribution. Therefore, $Q_{if}^{(\mathrm{SDS}-4\mathrm{B})\mp}$ can be written using $T_{if}^{(\mathrm{SDS}-4\mathrm{B})\mp}$ without the phases $(\mu v\rho)^{2i\tilde{v}_{f,i}}$:

$$Q_{if}^{(\mathrm{SDS}-4\mathrm{B})\mp}(a_0^2) = \int \mathrm{d}\boldsymbol{\eta} \left| \frac{T_{if}^{(\mathrm{SDS}-4\mathrm{B})\mp}(\boldsymbol{\eta})}{2\pi v} \right|^2, \tag{60}$$

$$T_{if}^{(\mathrm{SDS}-4\mathrm{B})-}(\boldsymbol{\eta}) = N(v) \iiint \mathrm{d}\boldsymbol{x}_1 \mathrm{d}\boldsymbol{x}_2 \mathrm{d}\boldsymbol{R} \, (vR - \boldsymbol{v} \cdot \boldsymbol{R})^{i\xi} \mathcal{D}\mathcal{K}^-_{if}, \tag{61}$$

$$T_{if}^{(\mathrm{SDS}-4\mathrm{B})+}(\boldsymbol{\eta}) = N(v) \iiint \mathrm{d}\boldsymbol{s}_1 \mathrm{d}\boldsymbol{s}_2 \mathrm{d}\boldsymbol{R} \, (vR + \boldsymbol{v} \cdot \boldsymbol{R})^{-i\xi} \mathcal{D}\mathcal{K}^+_{if}, \tag{62}$$

$$\mathcal{K}^-_{if} = \mathcal{P}_{12}\varphi^\star_f(\boldsymbol{s}_1, \boldsymbol{s}_2)\,_1F_1(iv_{\mathrm{T}}, 1, ivx_1 + i\boldsymbol{v} \cdot \boldsymbol{x}_1)\left[ Z_{\mathrm{P}}\left(\frac{1}{R} - \frac{1}{s_2}\right)\varphi_i(\boldsymbol{x}_1, \boldsymbol{x}_2) \right.$$

$$\left. - \frac{1}{b}\boldsymbol{\nabla}_{x_1}\varphi_i(\boldsymbol{x}_1, \boldsymbol{x}_2) \cdot \boldsymbol{\nabla}_{s_1} \right]\,_1F_1(iv_{\mathrm{P}}, 1, ivs_1 + i\boldsymbol{v} \cdot \boldsymbol{s}_1), \tag{63}$$

$$\mathcal{K}^+_{if} = \mathcal{P}_{12}\varphi_i(\boldsymbol{x}_1, \boldsymbol{x}_2)\,_1F_1(iv_{\mathrm{P}}, 1, ivs_1 + i\boldsymbol{v} \cdot \boldsymbol{s}_1)\left[ Z_{\mathrm{T}}\left(\frac{1}{R} - \frac{1}{x_2}\right)\varphi^\star_f(\boldsymbol{s}_1, \boldsymbol{s}_2) \right.$$

$$\left. - \frac{1}{a}\boldsymbol{\nabla}_{s_1}\varphi^\star_f(\boldsymbol{s}_1, \boldsymbol{s}_2) \cdot \boldsymbol{\nabla}_{x_1} \right]\,_1F_1(iv_{\mathrm{T}}, 1, ivx_1 + i\boldsymbol{v} \cdot \boldsymbol{x}_1), \tag{64}$$

$$\left.\begin{aligned}\mathcal{D} &\equiv e^{i\boldsymbol{k}_i\cdot\boldsymbol{r}_i + i\boldsymbol{k}_f\cdot\boldsymbol{r}_f} = e^{i\boldsymbol{\alpha}\cdot(\boldsymbol{s}_1+\boldsymbol{s}_2)+i\boldsymbol{\beta}\cdot(\boldsymbol{x}_1+\boldsymbol{x}_2)}\\ &= e^{2i\boldsymbol{\beta}\cdot\boldsymbol{R}-i\boldsymbol{v}\cdot(\boldsymbol{s}_1+\boldsymbol{s}_2)} = e^{-2i\boldsymbol{\alpha}\cdot\boldsymbol{R}-i\boldsymbol{v}\cdot(\boldsymbol{x}_1+\boldsymbol{x}_2)}\end{aligned}\right\}, \tag{65}$$

$$\left.\begin{aligned}\boldsymbol{\alpha} &= \frac{\boldsymbol{\eta} - v^+\hat{\boldsymbol{v}}}{2}, \quad \boldsymbol{\beta} = -\frac{\boldsymbol{\eta} + v^-\hat{\boldsymbol{v}}}{2}, \quad \boldsymbol{\alpha} + \boldsymbol{\beta} = -\boldsymbol{v}\\ v^+ &= v + \frac{\Delta\varepsilon}{v}, \quad v^- = v - \frac{\Delta\varepsilon}{v}, \quad \Delta\varepsilon = \varepsilon_f^{\mathrm{P}} - \varepsilon_i^{\mathrm{T}}\end{aligned}\right\}, \tag{66}$$

$$N(v) = N(v_{\mathrm{T}})N^{\star}(v_{\mathrm{P}}). \tag{67}$$

In the above expressions, the quantity $\boldsymbol{\eta}$ is the transverse momentum transfer vector, lying in the XOY plane and thus being orthogonal to the incident velocity $\boldsymbol{v}$ which is, as stated, in the Z-direction of the XOYZ system of reference (thus $\boldsymbol{\eta} \cdot \boldsymbol{v} = 0$).

## 2.3 The independent particle method and the CDW-3B-IPM

As stated, the CDW-3B-IPM for double capture by heavy nuclei from multi-electron targets is based on the CDW-3B method for single capture from the same atoms. To complement our earlier general remarks from Sect. 1 on the CDW-3B-IPM for double capture, we give here some more specific details deemed necessary for the general reader. To that end, we first recall the main working formulae of the CDW-3B method on $Q$ for electron capture by heavy nuclei from hydrogen-like targets. This pure three-body collision is symbolized as:

$$Z_{\mathrm{P}} + (Z_{\mathrm{T}}, e)_i \longrightarrow (Z_{\mathrm{P}}, e)_f + Z_{\mathrm{T}}. \tag{68}$$
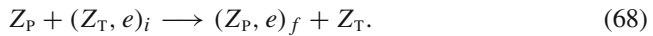
In the eikonal limit of large nuclear masses ($M_{\mathrm{P,T}} \gg 1$) and small scattering angles, the fully quantum-mechanical version of the prior form of the total cross section $Q$ in the CDW-3B method for (68) reads as [30]:

$$Q_{if}^{\mathrm{(CDW-3B)-}}(a_0^2) = \int \mathrm{d}\boldsymbol{\eta} \left| \frac{T_{if}^{\mathrm{(CDW-3B)-}}(\boldsymbol{\eta})}{2\pi v} \right|^2. \tag{69}$$

The transition amplitude $T_{if}^{\mathrm{(CDW-3B)-}}(\boldsymbol{\eta})$ depends on the transverse momentum transfer $\boldsymbol{\eta}$ and for $\hat{\boldsymbol{v}} \parallel \hat{\mathbf{Z}}$ it reads as:

$$T_{if}^{\mathrm{(CDW-3B)-}}(\boldsymbol{\eta}) = -\frac{1}{b}N(v)I , \quad I = \boldsymbol{J} \cdot \boldsymbol{K}, \tag{70}$$

$$\boldsymbol{J} = \int \mathrm{d}\boldsymbol{x} \, \mathrm{e}^{i\boldsymbol{p}\cdot\boldsymbol{x}} \, {}_1F_1(iv_{\mathrm{T}}, 1, ivx + i\boldsymbol{v}\cdot\boldsymbol{x})\nabla_x\varphi_i(\boldsymbol{x}), \tag{71}$$

$$\boldsymbol{K} = \int \mathrm{d}\boldsymbol{s} \, \mathrm{e}^{i\boldsymbol{q}\cdot\boldsymbol{s}}\varphi_f^{\star}(\boldsymbol{s})\nabla_{s1}F_1(iv_{\mathrm{P}}, 1, ivs + i\boldsymbol{v}\cdot\boldsymbol{s}), \tag{72}$$

$$\left.\begin{array}{l} \boldsymbol{p} = -\boldsymbol{\eta} - \tilde{v}^-\hat{\boldsymbol{v}}, \quad \boldsymbol{q} = \boldsymbol{\eta} - \tilde{v}^+\hat{\boldsymbol{v}}, \quad \boldsymbol{p} + \boldsymbol{q} = -\boldsymbol{v} \\[6pt] \tilde{v}^- = \dfrac{v}{2} - \dfrac{\Delta\tilde{\varepsilon}}{v}, \quad \tilde{v}^+ = \dfrac{v}{2} + \dfrac{\Delta\tilde{\varepsilon}}{v}, \quad \Delta\tilde{\varepsilon} = \tilde{\varepsilon}_f^{\mathrm{P}} - \tilde{\varepsilon}_i^{\mathrm{T}} \end{array}\right\}, \tag{73}$$

where $N(v)$ is given by (67) with the same Sommerfeld parameters $v_{\mathrm{P}}$ and $v_{\mathrm{T}}$ as in (41) and (52). In process (68), vectors $\boldsymbol{x}$ and $\boldsymbol{s}$ connect the electron $e$ to the target and projectile nuclear charges $Z_{\mathrm{P}}$ and $Z_{\mathrm{T}}$, respectively. For this collision, the wave functions $\varphi_i(\boldsymbol{x})$ and $\varphi_f(\boldsymbol{s})$, alongside the corresponding energies $\tilde{\varepsilon}_i^{\mathrm{T}}$ and $\tilde{\varepsilon}_f^{\mathrm{P}}$, with the standard triple of the quantum numbers $i = \{n_i l_i m_i\}$ and $f = \{n_f l_f m_f\}$, describe

the initial and final bound states of the hydrogen-like systems $(Z_T, e)_i$ and $(Z_P, e)_f$ in the entrance and exit channel, respectively.

As it stands, the transition amplitude $T_{if}^{(CDW-3B)-}$ from (70) is purely electronic. For computations of $Q$, the phase $(\mu v \rho)^{2i\nu_{PT}}$, as the only remnant of the presence of the Coulomb internuclear potential $V_{PT}$, is dropped from $T_{if}^{(CDW-3B)-}$. This is similar to the neglect of the $\rho$−dependent phases in $T_{if}^{(SDS-4B)-}$ from (61), when computing $Q_{if}^{(SDS-4B)-}$ from (60). In $(\mu v \rho)^{2i\nu_{PT}}$, the reduced mass $\mu$ is from (59) and $\nu_{PT} = Z_P Z_T / v$ is the Sommerfeld parameter for the internuclear potential $V_{PT} = Z_P Z_T / R$. The omitted phase $(\mu v \rho)^{2i\nu_{PT}}$ does not contribute to $Q$, but it needs to be reintroduced for differential cross sections [11, 31].

Vectors $\boldsymbol{\eta}$ and $\boldsymbol{\rho}$ are the two canonical conjugate variables. As such, for the given two functions, if one of them depends on $\boldsymbol{\eta}$ and the other on $\boldsymbol{\rho}$, they can be interconnected by the direct and inverse two-dimensional Fourier integrals. Taking these two functions to be the transition amplitudes $T_{if}^{(CDW-3B)-}(\boldsymbol{\eta})$ and $\mathcal{A}_{if}^{(CDW-3B)-}(\boldsymbol{\rho})$, it follows:

$$\mathcal{A}_{if}^{(CDW-3B)-}(\boldsymbol{\rho}) = \frac{1}{2\pi} \int d\boldsymbol{\eta} \, e^{i\boldsymbol{\eta}\cdot\boldsymbol{\rho}} T_{if}^{(CDW-3B)-}(\boldsymbol{\eta}), \qquad (74)$$

where, as before, $\boldsymbol{\rho} \cdot \boldsymbol{v} = 0$ and $\boldsymbol{\eta} \cdot \boldsymbol{v} = 0$. The total cross section $Q$ could alternatively be computed by integrating $\left| \mathcal{A}_{if}^{(CDW-3B)-}(\boldsymbol{\rho}) \right|^2$ over $\boldsymbol{\rho}$. Advantageously, by virtue of the Parseval relation, the result is exactly the same as that due to the corresponding integration of $T_{if}^{(CDW-3B)-}(\boldsymbol{\eta})$ over $\boldsymbol{\eta}$ in $Q_{if}^{(CDW-3B)-}$ from (69).

For any quantum numbers $\{n_{i,f} l_{i,f} m_{i,f}\}$, the general analytical expressions of $T_{if}^{(CDW-3B)-}(\boldsymbol{\eta})$ from (70) for the pure three-body problem (68) as well as for multielectron targets in the Roothan-Hartree-Fock (RHF) formalism are available in the literature alongside the corresponding computer codes [32–38]. In the RHF framework [11], only one electron is considered as active, whereas all the other electrons are viewed as passive (i.e. they occupy the same orbitals before and after the collision). These analytical expressions for $T_{if}^{(CDW-3B)-}(\boldsymbol{\eta})$ permit deduction of the general expressions for $\mathcal{A}_{if}^{(CDW-3B)-}(\boldsymbol{\rho})$ by means of the inverse Fourier integral [31].

An explicit expression of $\mathcal{A}_{if}^{(CDW-3B)-}(\boldsymbol{\rho})$ for the ground-to-ground state transition ($i = 1s, \ f = 1s$) in process (68) can be found in Ref. [31] as a compact formula with two one-dimensional numerical quadratures. The same formula contains an appropriate adaptation for an effective target nuclear charge. A linear combination of this type of the $\rho$−dependent transition amplitudes allows applications to single capture by heavy nuclei from multi-electron targets in the RHF formalism, as illustrated in Ref. [31] for differential cross sections $(d/d\Omega) Q_{if}^{(CDW-3B)-}$.

For the hydrogen-like and multi-electron systems, both $T_{if}^{(CDW-3B)-}(\boldsymbol{\eta})$ and $\mathcal{A}_{if}^{(CDW-3B)-}(\boldsymbol{\rho})$ treat the motions of all the three active particles quantum-mechanically. Therefore, these two transition amplitudes are fully quantum-mechanical in their common origin. They involve the time-independent relation $\boldsymbol{R} = \boldsymbol{\rho} + v\hat{Z}\,\hat{\boldsymbol{v}} \parallel \hat{\boldsymbol{Z}}$ only geometrically. This should not be confused with the projectile classical motion

along a time-dependent rectilinear trajectory $\boldsymbol{R}(t) = \boldsymbol{\rho} + \boldsymbol{v}t$, characterized by an impact parameter $\boldsymbol{\rho}$ and a constant velocity $\boldsymbol{v}$. However, it is well-known that, in the eikonal limit $(1/M_{\mathrm{P,T}} \ll 1$, small scattering angles), the full quantum-mechanical and semi-classical impact parameter formalisms are completely equivalent and they give the same cross sections.

In the time-dependent semi-classical IPM, only the electronic degrees of freedom are quantized, whereas the nuclear motions are described classically by the mentioned straight lines. Thus, the discussed quantum-mechanical quantity $\mathcal{A}_{if}^{(\mathrm{CDW-3B})-}(\boldsymbol{\rho})$ for single capture can acquire its alternative and equivalent interpretation in the IPM as the semi-classical impact parameter dependent transition amplitude. With such an interpretation of $\mathcal{A}_{if}^{(\mathrm{CDW-3B})-}(\boldsymbol{\rho})$, its squared absolute value gives the impact parameter dependent transition probability for single capture.

Moreover, in the independent electron formalism, the product of these two impact parameter dependent probabilities for two separate and uncorrelated capture events of each electron from a helium-like or multi-electron targets by ions defines the probability for double capture. An integration of such a product of the single capture probabilities over the impact parameters yields a total cross section $Q$ for double capture in the CDW-3B-IPM from the present computations, similarly to the earlier studies [39, 40].

These probabilities are real-valued quantities and, therefore, their products in the CDW-3B-IPM are void of any phase interference. That is why the CDW-3B-IPM for double capture (or multiple capture) is an inherently semi-classical theory. The prime signature of quantum mechanics is phase interference of physical quantities. Phase interference is abundant in e.g. the fully quantum-mechanical transition amplitudes $T_{if}^{(\mathrm{SDS-4B})\pm}(\boldsymbol{\eta})$ for double capture in the SDS-4B method.

## 3 Results and analysis

We will now exemplify the general case of double capture in process (1) by considering its homo-nuclear specification ($Z_{\mathrm{T}} = Z_{\mathrm{P}} = 2$) for the ground-to-ground state transition:

$$^{4}\mathrm{He}^{2+} + {}^{4}\mathrm{He}(1s^2) \longrightarrow {}^{4}\mathrm{He}(1s^2) + {}^{4}\mathrm{He}^{2+}. \tag{75}$$
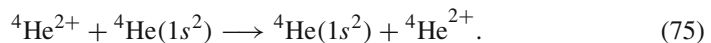
Some of the measured cross sections $Q(\mathrm{ground})$ versus impact energy $E$ reported in the literature [41, 42] are for ground-to-ground transition in the resonant collision (75). However, the great majority of the experimental data [43–56] are for the sum of ground-to-ground state and ground-to-excited state transitions. Here, the final excited states are considered as non-autoionizing. In other words, the summed cross sections $Q(\Sigma) = Q(\mathrm{ground}) + Q(\mathrm{excited})$ correspond to the process:

$$^{4}\mathrm{He}^{2+} + {}^{4}\mathrm{He}(1s^2) \longrightarrow {}^{4}\mathrm{He}(\Sigma) + {}^{4}\mathrm{He}^{2+}. \tag{76}$$
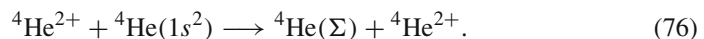
The theoretical results are only for process (75). They are due to the prior forms of the semi-classical treatment from the CDW-3B-IPM and to the quantum-mechanical

formalism from the SDS-4B and CDW-4B methods. Our main emphasis here is on comparing the SDS-4B method and CDW-3B-IPM in relation to the experimental data. For completeness, however, also added is the CDW-4B method to these comparisons as a complement to Ref. [6] on similar evaluations.

The helium ground-state wave functions $\varphi_{i,f}$ that have frequently been used for studies on rearrangement ion-atom collisions contain several parameters, e.g. one: Hylleraas [57], two: Silverman *et al.* [58], three: Green *et al.* [59] or four: Löwdin [60], etc. The parameters from Refs. [57–59] are variational, whereas those from Ref. [60] stem from fitting a few Slater-type orbitals (STOs) to the known tabulated values of the RHF wave functions. Also often employed for electron capture by ions from many atoms [11] were the general analytical STOs for the RHF wave functions with the variational parameters determined by Clementi and Roetti [61]. In Ref. [5] on double capture in process (75), cross sections $Q$ were computed with the one-to-four-parameter wave functions [57–60]. For $Q$, the most noticeable differences among these four functions were at high energies $E$.

The present choices of $\varphi_{i,f}$ are also within this type of wave functions in the case of helium atoms. Thus, in the CDW-3B-IPM, two selections of the initial state wave function $\varphi_i$ are made. They are associated with one and five parameters from Refs. [57] (Hylleraas) and [61] (Clementi and Roetti), respectively. For both choices of $\varphi_i$, the final state wave function $\varphi_f$ is taken to be that of Hylleraas [57]. In the case of the SDS-4B and CDW-4B methods, both $\varphi_i$ and $\varphi_f$ are due to Hylleraas [57].

To illustrate, two figures are shown both dealing with total cross sections $Q$ versus $E$ for double capture in the $\alpha - $ He collisions as in processes (75) and (76). Figure 1 for the CDW-3B-IPM alone is on the sensitivity of $Q$ to the mentioned two choices of $\varphi_i$ considered at $E = 80 - 8000$ keV. The same range of $E$ is also covered in Fig. 2, where the SDS-4B and CDW-4B methods are compared with the CDW-3B-IPM as well as with the existing measured cross sections $Q$.

In Fig. 1, the full curve ($D_1$) is for $\varphi_{i,f}$ of Hylleraas [57]. The dashed curve ($D_2$) is for the RHF wave function $\varphi_i$ of Clementi and Roetti [61] and for $\varphi_f$ of Hylleraas [57]. Below about 1500 keV, the full curve overestimates the dashed curve, whereas thereafter the converse is true. This can be understood from the arguments that run as follows. At high impact energies, capture is more probable (with the ensuing larger values of $Q$) for the greater momentum components of the initial and final bound-state wave functions. Regarding the equivalent coordinate and momentum representations of the given bound-state wave function, larger momenta correspond to smaller spatial distances (the latter relate to better compactness/confinement of the pertinent atomic orbitals).

Consequently, the more compact the bound-state wave function is in the coordinate representation, the more probable the high-energy capture becomes. The multi-configuration RHF wave function [61] is more compact than the single configuration of Hylleraas [57]. Therefore, with increasing $E$, the larger $Q$ should ensue with the multi-configuration than with the single-configuration $\varphi_i$ of helium. This is confirmed in Fig. 1 at $E > 1500$ keV, where the dashed curve for the five-configurations [61] lies above the full curve for one-configuration [57].

To have an indication of the relative contributions of the helium ground and excited states in the exit channel, a few relevant measured cross sections $Q$ (plotted as symbols)
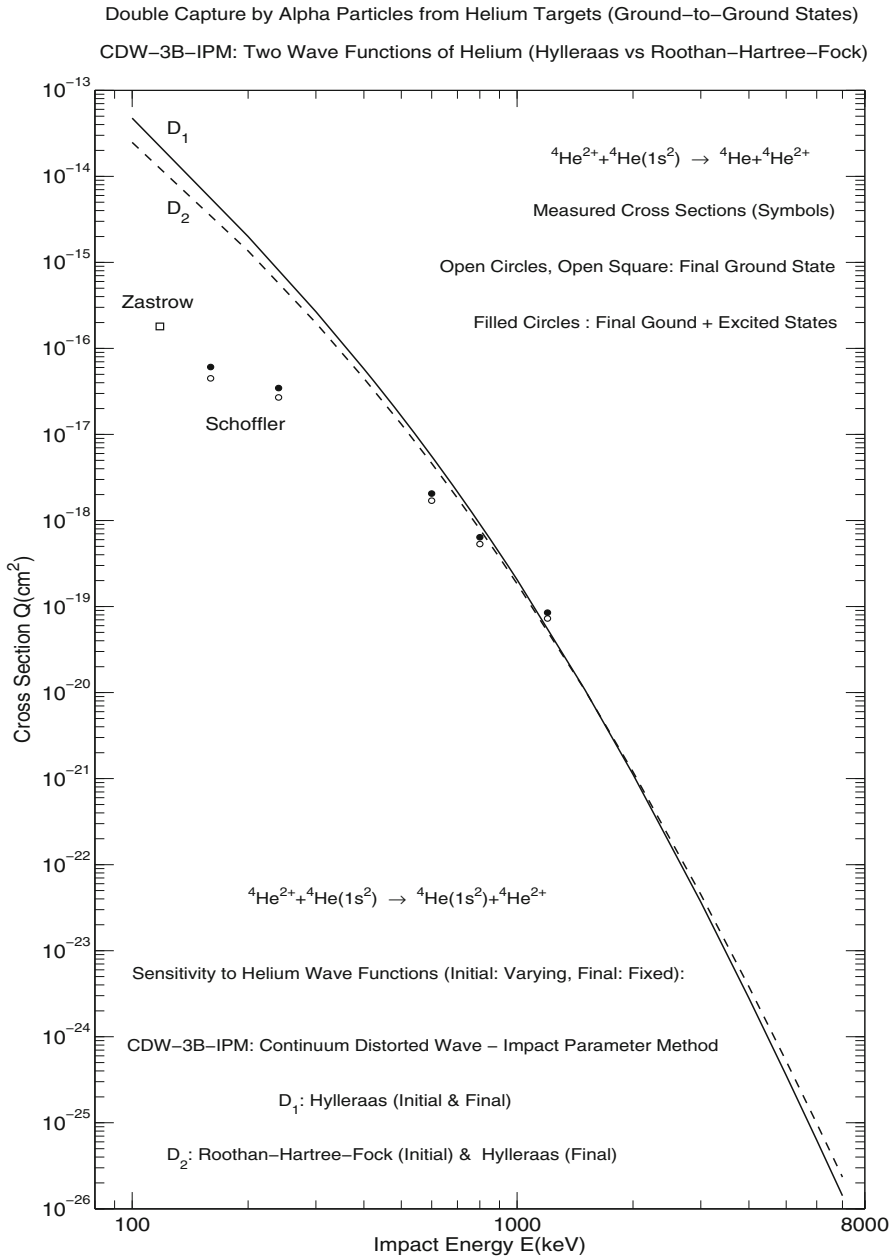
**Fig. 1** Total cross sections $Q(\text{cm}^2)$ versus impact energy $E(\text{keV})$ for double capture in the $\alpha - \text{He}$ collisions. The dashed and full curves are the present theoretical data from the CDW-3B-IPM for process (75). Both curves describe the final ground state of helium by the one-parameter wave function of Hylleraas [57]. As to the wave function of the initial ground state of helium, the full and dashed curves are for the one-parameter single configuration of Hylleraas [57] and the RHF five-parameter multi-configuration of Clementi and Roetti [61], respectively. Experimental data are for process (75): □ [41] (JET, Joint European Torus, within the ITER, International Thermonuclear Experimental Reactor), ○ [42] (COLTRIMS, cold target recoil ion momentum spectroscopy) and for process (76): ● [42]. For details, see the main text (color online)
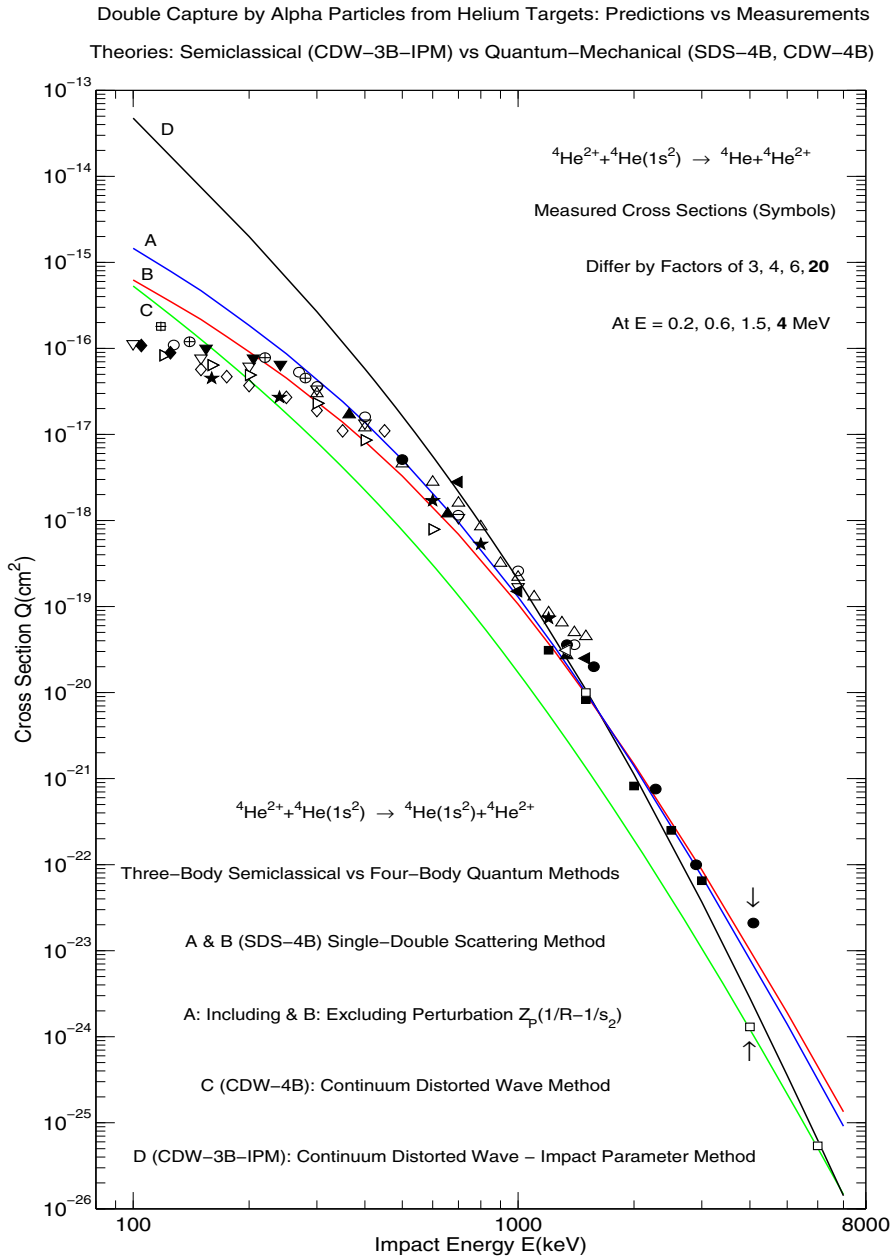
**Fig. 2** Total cross sections $Q(\text{cm}^2)$ versus impact energy $E(\text{keV})$ for double capture in the $\alpha - $He collisions. The present theoretical results are for process (75) for which the initial and final ground state helium wave functions are represented by the one-parameter single configurations of Hylleraas [57]: SDS-4B (curves A, B), CDW-4B (curve C) and CDW-3B-IPM (curve D). For process (75), the only experimental result plotted here is that of Zastrow *et al*. [41]. All the remaining measured cross sections are for capture into any final bound non-autoionizing state of helium. Experimental data: ⊞ [41], ★ [42]. ◇ [43], △ [44], ▽ [45], ■ [46], ▲ [47], ▼ [48], ◆ [49], ○ [50], ◀ [51], ◁ [52], ▷ [53], ⊕ [54], □ [55], ● [56], For details, see the main text (color online)

are displayed in Fig. 1. Herein, open symbols [41, 42] are the experimental data $Q$ for the final ground state of helium in process (75). The full symbols are for the sum of the ground and all the excited states of helium [42] in process (76). The open and full symbols due Schöffler *et al.* [42] show that all the final excited states of helium give a relatively small contribution. This justifies comparing the theoretical results for (75) with the experimental data for (76), as has been done earlier [5, 6] and will be followed presently, as well.

The results for process (75) in the CDW-3B-IPM (Fig. 1) largely overestimate the corresponding experimental data at intermediate energies, but are in good agreement with the measured cross sections $Q$ at higher $E$. Note that, regarding the juxtaposition of the theoretical predictions and measurements, Fig. 1 is a preview and a more detailed comparison is deferred to Fig. 2. Nevertheless, regarding process (75), it can be seen in Fig. 1 that, if the measured cross sections $Q$ of Schöffler *et al.* [42] are extrapolated to lower $E$, they would underestimate the single datum $Q$ at 117 keV of Zastrow *et al.* [41] by about a factor of three.

In Fig. 2, the SDS-4B (A, B) and CDW-4B (C) methods as well as the CDW-3B-IPM (D) are compared with the available experimental data [41–56]. Herein, all the lines A-D are for $\varphi_{i,f}$ of Hylleraas [57]). The lines A and B from the SDS-4B method are with and without the perturbation $Z_P(1/R - 1/s_2)$, respectively. It is observed that the CDW-3B-IPM as well as the CDW-4B and SDS-4B methods predict very different energy dependence of $Q$ as well as the magnitudes of the computed total cross sections.

For example, at 100 keV, the discrepancy in the magnitude of $Q$ between the CDW-3B-IPM (D) and the SDS-4B (A, B) or the CDW-4B (C) methods is about a factor of 20 or 30. A large overestimation of the experimental data by the CDW-3B-IPM (D) persists up to about 600 keV. On the other hand, the SDS-4B method (A, B) is in good agreement with the measurements above 200 keV. The difference between the lines A and B from the SDS-4B method is noticeable, but both predictions are acceptable, especially given that there is a considerable scatter or dispersion of the experimental data on $Q$ from different measurements. Perturbation $Z_P(1/R - 1/s_2)$ is absent not only from the SDS-4B method (B), but also from the CDW-3B-IPM (D).

Above about 3500 keV, the status of the theories and measurements is inconclusive. For instance, at about 4000 keV, the measured cross sections of Schuch *et al.* [55] and Afrosimov *et al.* [56] differ by a factor of about 20. The CDW-3B-IPM (D) and CDW-4B (C) method are close to the data from Ref. [55]. However, the SDS-4B method (A, B) is near the data from Ref. [56]. Overall, it follows from Fig. 2 that the SDS-4B method exhibits favorable agreement with most experimental data and, moreover, it is clearly superior to both the CDW-3B-IPM and CDW-4B method. A detailed discussion on the comparison between the SDS-4B (A) and CDW-4B (C) methods as well as between the lines A and B from the SDS-4B method can be found in Ref. [6].

## 4 Discussion and conclusion

This study is on second-order distorted wave perturbative theories for predictions of total cross sections $Q$ for two-electron capture by heavy nuclei from helium-like targets

at intermediate and high impact energies $E$. For these collisions, this type of distorted wave theories employs the full Coulomb wave functions for electrons to describe their continuum intermediate states in the external fields of nuclei. Such electronic ionization continua are associated with double scatterings of the given electron on two nuclei as reminiscent of the Thomas classical billiard-type two-step collisional mechanism.

The complex-valued continuum Coulomb wave functions are highly oscillatory. Interference in the product of two or more such Coulomb waves within the transition amplitudes can significantly influence the probabilities for double charge exchange. The more Coulomb waves in such products, the more destructive interferences and the lower the double capture transition probability. Therefore, this 'multiplication effect' in distortions associated with the electronic full Coulomb waves can lead to an over-account of intermediate ionization continua with a repercussion on the chance for double capture.

The electronic distortion effects are included differently in various perturbative methods. For instance, the CDW-4B method is completely symmetric in regard to both electrons in two channels. It has two full Coulomb wave functions in each channel. These four electronic full Coulomb waves interfere strongly through their product in the transition amplitudes and, therefore, can notably reduce the probabilities for double charge exchange. This can further be exacerbated by the fact that the CDW-4B method describes both electrons as being simultaneously transferred from the target to the projectile by the identical mechanism. The chance for such an event to happen is small due to the underlying requirement that the two electrons come to nearly the same place at almost the same time.

On the other hand, in the SDS-4B method for double capture, there is one full electronic Coulomb wave function per channel. Therefore, the 'multiplication effect' of the full Coulomb waves for electrons is relatively milder. As such, the ensuing interference reduction could enhance the probability for two-electron transfer. Yet another reason for this expected enhancement is a less restrictive requirement for transitions, since this method combines two different mechanisms, single scattering (one-step) for one electron and double scattering (two-steps) for the other electron from a helium-like target. Such two collisional pathways can occur through the more relaxed conditions as the two electrons need not necessarily be in the same place at the same time.

In order to capture an electron (say $e_1$) via single scatterings (one-step), an incident nucleus of charge $Z_P$ needs to come close to a helium-like target. However, should the other electron ($e_2$) be transferred to the projectile by double collisions (once on each nucleus), there would be no prerequisite for $Z_P$ to be near the target. Being e.g. far away from the target nuclear charge $Z_T$, the projectile can still impart some of its energy to electron $e_2$, which could subsequently scatter on $Z_T$ and finally get captured by $Z_P$ (the Thomas mechanism).

Within the semi-classical impact parameter dependent theories, the CDW-3B-IPM for the underlying three-body ingredient of double charge exchange also has two electronic full Coulomb wave functions (one per channel). This feature too should increase the probability for double capture. Since both the CDW-3B-IPM and SDS-4B method have two electronic full Coulomb waves, it is intriguing to find out whether

these two theories could yield some comparable results for $Q$ at least at some energies $E$. Of equal interest is to determine at which energies $E$ there could be some significant differences between the CDW-3B-IPM and SDS-4B method. The present study was set to answer these queries and, most importantly, to assess the overall performance of these two methods relative to the existing experimental data.

The CDW-3B-IPM computes the probability $P_1$ for capture of $e_1$ with no concern whatsoever about the fate of $e_2$. If double capture is to be investigated, the probability $P_2$ for transfer of $e_2$ should also be evaluated in the same manner to obtain the joint probability $P_1 P_2$ for the two independent uncorrelated events. Hence, the CDW-3B-IPM accounts for the participation of two electrons to double capture through a combinatorial calculus in the spirit of an independent particle modeling.

By definition of a three-body theory, the CDW-3B-IPM, has no room to accommodate for the simultaneous presence of two electrons on an active, dynamical level in the Schrödinger equations for the total scattering wave function. However, the SDS-4B method, as a fully correlated quantum-mechanical four-body theory, considers both electrons $e_{1,2}$ as being actively present throughout the entire collision process.

The concerted participation of electrons $e_{1,2}$ to the transition amplitude for double capture is through the electron initial/final distorting potentials and distorted waves. In particular, the distorted waves include the electronic translation factors of $e_{1,2}$ that are of utmost importance at higher energies $E$. Therefore, it is of interest to assess the influence of these differences on the cross sections predicted by the SDS-4B method and the CDW-3B-IPM.

To address such issues, we computed total cross sections $Q$ as a function of impact energy $E$ at 80-8000 keV for double electron capture by alpha particles from the ground state of helium target atoms. It is shown that indeed there are energy regions where these two methods differ considerably (e.g. in the intermediate region below 600 keV), while elsewhere (e.g. at 600-3000 keV) they are reasonably concordant. However, overall, at most energies $E$, the experimental data definitely favor the SDS-4B method which, in this respect too, shows a clear superiority over the CDW-3B-IPM.

More comparisons are needed between the SDS-4B method and the available experimental data on double capture involving a number of other scattering aggregates. If such further tests prove favorable, it would be both interesting and useful to apply this theory to the collisions of relevance particularly to ion therapy of patients (irradiation of malignant cells from deep-seated tissue) and to hot ion plasma from nuclear fusion reactors. Importantly, two-electron transfer induced by multiply charged ions impacting on helium ($N^{q+} - He$, $Ne^{q+} - He$) are currently examined by means of charge exchange spectroscopy for plasma diagnostics in the Axially Symmetric Divertor Experiment (ASDEX) and its upgrade (ASDEXU) within the International Thermonuclear Experimental Reactor (ITER).

**Author contributions** The Author himself designed and performed all the work in this study.

**Data availibility** Data from this work can be made available to other researchers in this field upon request to the Author.

## Declarations

**Conflict of interest** The Author declares that he has no known competing funding, employment, financial or non-financial interests that could have appeared to influence the work reported in this paper.

## References

1. Dž. Belkić, Review of theories on ionization in fast ion-atom collisions with prospects for applications to hadron therapy. J. Math. Chem. **47**, 1366–1416 (2010)
2. Dž. Belkić, Double charge exchange in ion-atom collisions using distorted wave theories with two-electron continuum intermediate states in one or both scattering channels. J. Math. Chem. **57**, 1–58 (2019)
3. Dž. Belkić, Total cross sections in five methods for two-electron capture by alpha particles from helium: CDW-4B, BDW-4B, BCIS-4B, CDW-EIS-4B and CB1-4B. J. Math. Chem. **58**, 1133–1176 (2020)
4. Dž. Belkić, Distorted wave theories with correct boundary conditions for double charge exchange in ion-atom collisions at intermediate and high energies. Adv. Quantum Chem. **86**, 223–296 (2022)
5. Dž. Belkić, High-energy two-electron transfer in ion-atom collision. J. Math. Chem. **61**, 177–184 (2023)
6. Dž. Belkić, Various mechanisms for double capture from helium targets by alpha particles. J. Math. Chem. **61**, 2019–2044 (2023)
7. Dž. Belkić, Single charge exchange in collisions of energetic nuclei with biomolecules of interest to ion therapy. Z. Med. Phys. **31**, 122–144 (2021)
8. Dž. Belkić, One electron-capture in collisions of fast nuclei with biomolecules of relevance to ion therapy. Adv. Quantum Chem. **84**, 267–345 (2021)
9. J. Dollard, Asymptotic convergence and Coulomb interactions. J. Math. Phys. **5**, 729–738 (1964)
10. I.M. Cheshire, Continuum distorted wave approximation; resonant charge transfer by fast protons in atomic hydrogen. Proc. Phys. Soc. **84**, 89–98 (1964)
11. Dž. Belkić, R. Gayet, A. Salin, Electron capture in high-energy ion-atom collisions. Phys. Rep. **56**, 279–369 (1979)
12. Dž. Belkić, *Principle of Quantum Scattering Theory* (Taylor & Francis, London, 2004)
13. Dž. Belkić, *Quantum Theory of High-Energy Ion-Atom Collisions* (Taylor & Francis, London, 2008)
14. Dž. Belkić, *State-of-the-Art Reviews on Energetic Ion-Atom and Ion-Molecule Collisions* (World Scientific Publishing, Singapor, 2019)
15. Dž. Belkić, S. Saini, H. Taylor, A critical test of first-order theories for electron transfer in collisions between multicharged ions and atomic hydrogen. Phys. Rev. A **36**, 1601–1617 (1987)
16. Dž. Belkić, S. Saini, H. Taylor, General results for hydrogenlike and multielectron targets, First-order theory for charge exchange with correct boundary conditions. Phys. Rev. A **36**, 1991–2006 (1987)

17. F. Busnengo, A.E. Martínez, R.D. Rivarola, Single electron capture from He targets. J. Phys. B **29**, 4193–4205 (1996)

18. L. Gulyás, P.D. Fainstein, T. Shirai, Extended description for electron capture in ion-atom collisions: application of model potentials within the framework of the continuum distorted wave theory. Phys. Rev. **65**, 052720 (2002)

19. Dž. Belkić, I. Mančev, Formation of H⁻ by double charge exchange in fast proton-helium collisions. Phys. Scr. **45**, 35–42 (1992)

20. Dž. Belkić, Importance of intermediate ionization continua for double charge exchange at high energies. Phys. Rev. A **47**, 3824–3844 (1993)

21. Dž. Belkić, Symmetric double charge exchange in fast collisions of bare nuclei with helium-like atomic systems. Phys. Rev. A **47**, 189–200 (1993)

22. Dž. Belkić, Two-electron capture from helium-like atomic systems by completely stripped projectiles. J. Phys. B **26**, 497–508 (1993)

23. Dž. Belkić, Double charge exchange at high impact energies. Nucl. Instrum. Meth. Phys. Res. B **86**, 62–81 (1994)

24. A.E. Martínez, R.D. Rivarola, R. Gayet, J. Hanssen, Double electron capture theories: second order contributions. Phys. Scr. **T80**, 124–127 (1999)

25. Dž. Belkić, Review of theories on ionization in fast ion-atom collisions with prospects for applications to hadron therapy. J. Math. Chem. **47**, 1366–1419 (2010)

26. D.E. Post, D.R. Mikkelsen, R.A. Hulse, L.D. Stewart, J.C. Weisheit, Techniques for Measuring the Alpha-Particle Distribution in Magnetically Confined Plasmas, Princeton Plasma Physics Laboratory, Report PPPL-1592 (1979) http://digital.library.unt.edu/ark:/67531/metadc1099819/m1/1/

27. R. Olson, Electron capture and ionisation in H⁺, He²⁺ + Li collisions. J. Phys. B **15**, L163–L167 (1982)

28. A.S. Schachter, J.W. Stearns, W.S. Cooper, A Neutral Beam Diagnostic for Fast Confined Alpha Particles in a Burning Plasma: Application on CIT, Lawrence National Laboratory, Report LBL-24235, (1987) https://escolarship.org/uc/item/982317js

29. H. Tawara, Roles of Atomic and Molecular Processes in Fusion Plasma Researches, Japan National Institute for Fusion Science, Report NIFS-DATA-25 (1995) http://nifs.ac.jp/report/NIFS-DATA-025.pdf

30. Dž. Belkić, Projectile charge dependence of electron-capture cross sections. J. Phys. B **10**, 1933–1943 (1977)

31. Dž. Belkić, A. Salin, Differential cross sections for charge exchange at high energies. J. Phys. B **11**, 3905–3911 (1978)

32. Dž. Belkić, Bound-free non-relativistic transition form factors in atomic hydrogen. J. Phys. B **14**, 1907–1914 (1981)

33. Dž. Belkić, Analytical results for Coulomb integrals with hydrogenic and Slater-type orbitals. J. Phys. B **16**, 2773–2784 (1983)

34. Dž. Belkić, Electron transfer from hydrogenlike atoms to partially and completely stripped projectiles: CDW approximation. Phys. Scr. **43**, 561–571 (1991)

35. Dž. Belkić, Vector spherical harmonics and scattering integrals. Phys, Scr. **45**, 9–17 (1992)

36. Dž. Belkić, R. Gayet, A. Salin, Computation of total cross-sections for electron capture in high energy ion-atom collisions. Comput. Phys. Commun. **23**, 153–167 (1981)

37. Dž. Belkić, R. Gayet, A. Salin, Computation of total cross sections for electron capture in high energy collisions: II. Comput. Phys. Commun. **30**, 193–205 (1983)

38. Dž. Belkić, R. Gayet, A. Salin, Computation of total cross sections for electron capture in high energy collisions: III. Comput. Phys. Commun. **32**, 385–397 (1984)

39. R. Gayet, R.D. Rivarola, A. Salin, Double electron capture by fast nuclei. J. Phys. B **14**, 2421–2427 (1981)

40. M. Ghosh, C.R. Mandal, S.C. Mukherjee, Single and double electron capture from lithium by fast α particles. J. Phys. B **18**, 3797–3803 (1985)

41. K.-D. Zastrow, M. O'Mullane, M. Brix, C. Giroud, A.G. Meigs, M. Proschek, H.P. Summers, Double charge exchange from helium neutral beams in a tokamak plasma. Plasma Phys. Control. Fusion **45**, 1747–1756 (2003)

42. M.S. Schöffler, J. Titze, L.Ph.H. Schmidt, T. Jahnke, N. Neumann, O. Jagutzki, H. Schmidt-Böcking, R. Dörner, I. Mančev, State-selective differential cross sections for single and double electron capture in He⁺,²⁺ − He and p − He collisions. Phys. Rev. A **79**, 064701 (2009). The corresponding total

cross sections, left out from this reference, can be found in an earlier report by the same authors: (arXiv:0711.4920v1 [physics.atom-ph]) 30 Nov 2007

43. S.K. Allison, Allison, Experimental results on charge-changing collisions of hydrogen and helium atoms and ions at kinetic energies above 0.2 keV. Rev. Mod. Phys. **30**, 1137–1168 (1958)

44. L.I. Pivovar, M.T. Novikov, V.M. Tubaev, Electron capture by helium ions in various gases in the 300–1500 keV energy range. J. Exp. Theor. Phys. JETP **15**, 1035–1039 (1962)

45. R.D. DuBois, Ionization and charge transfer in $He^{2+}$−rare gas collisions. II. Phys. Rev. A **36**, 2585–2593 (1987)

46. N.V. de Castro Faria, F.L. Freire Jr., A.G. de Pinho, Electron loss and capture by fast helium ions in noble gases. Phys. Rev. A **37**, 280–283 (1988)

47. V.S. Nikolaev, L.N. Fateeva, I.S. Dmitriev, Ya. A. Teplova, Capture of several electrons by fast multi-charged ions. J. Exp. Theor. Phys. JETP **14**, 67-74 (1962) [Zh. Eksp. Teor. Fiz. **41**, 89-99 (1961)]

48. K.H. Berkner, R.V. Pyle, J.W. Stearns, Single- and double-electron capture by 7.2 to 181 keV $^3He^{++}$ ions in He. Phys. Rev. **166**, 44–46 (1968)

49. J.E. Bayfield, G.A. Khayrallah, Electron transfer in keV-energy $^4He^{++}$ atomic collisions: I. Single and double electron transfer with He, Ar, $H_2$ and $N_2$. Phys. Rev. A **11**, 920–929 (1975)

50. E.W. McDaniel, M.R. Flannery, H.W. Ellis, F.L. Eisele, W. Pope, T.G. Roberts, Compilation of data relevant to rare-gas and rare-gas-monohalide excimer lasers. US Army Missile Research and Development Command, Redstone Arsenal, Alabama, Vol. I, Technical Report, No. H-78-1 (1977) https://www.army.mil/article/119547/research_center_paved_way_for_development

51. A. Itoh, M. Asari, F. Fukuzawa, Charge-changing collisions of 0.7–2.0 MeV helium beams in various gases. I. Electron capture. J. Phys. Soc. Jpn. **48**, 943–950 (1980)

52. I.S. Dmitriev, N.F. Vorob'ev, Zh.M. Konovalova, V.S. Nikolaev, V.N. Novozhilova, Ya.A. Teplova, Yu.A. Faĭnberg, Loss and capture of electrons by fast ions and atoms of helium in various media. J. Exp. Theor. Phys. JETP **57**, 1157-1164 (1983) [Zh. Eksp. Teor. Fiz. **84**, 1987-2000 (1983)]

53. M.E. Rudd, T.V. Goffe, A. Itoh, Ionization cross sections for 10–300-keV/amu and electron-capture cross sections for 50–150-keV/u $^3He^{2+}$ ions in gases. Phys. Rev. A **32**, 2128–2133 (1985)

54. R.D. DuBois, Ionization and charge transfer in $He^{2+}$-rare gas collisions. Phys. Rev. A **33**, 1595–1601 (1986)

55. R. Schuch, E. Justiniano, H. Vogt, G. Deco, N. Grün, Double electron capture by $He^{2+}$ from He at high velocity. J. Phys. B **24**, L133-138 (1991)

56. V.V. Afrosimov, D.F. Barash, A.A. Basalaev, N.A. Gushchina, K.O. Lozhkin, V.K. Nikulin, M.N. Panov, I.Yu. Stepanov, Single- and double-electron capture from many-electron atoms by $\alpha$ particles in the MeV energy range. J. Exp. Theor. Phys. JETP **77**, 554-561 (1993) [Zh. Eksp. Teor. Fiz. **104**, 3297-3310 (1993)]

57. E.A. Hylleraas, Neue Berechnung der Energie des Heliums im Grundzustande, sowie tiefsten Terms von Ortho-Helium. Z. Phys. **54**, 347–366 (1929)

58. J. Silverman, O. Platas, F.A. Matsen, Simple configuration-interaction wave functions. I. Two-electron ions: a numerical study. J. Chem. Phys. **32**, 1402–1406 (1960)

59. L.C. Green, M.M. Mulder, M.N. Lewis, J.W. Woll Jr., A discussion of analytic and Hartree–Fock wave functions for $1s^2$ configurations from $H^-$ to C. Phys. Rev. **93**, 757–761 (1954)

60. P.O. Löwdin, Studies of atomic self-consistent fields. I. Calculation of Slater functions. Phys. Rev. **90**, 120–125 (1953)

61. E. Clementi, C. Roetti, Roothaan–Hartree–Fock atomic wavefunctions: basis functions and their coefficients for ground and certain excited states of neutral and ionized atoms: $Z \leq 54$. At. Data Nucl. Data Tables **14**, 177–478 (1974)